Cover Page:

Lisa Duncan and Jessica Keister
Winterthur/University of Delaware Program in Art Conservation

IN PURSUIT OF REALITY: A TECHNICAL STUDY OF TWO OBSCURE PHOTOGRAPHIC PROCESSES OF THE 19TH CENTURY

Lisa Duncan and Jessica Keister
Winterthur/University of Delaware Program in Art Conservation

IN PURSUIT OF REALITY: A TECHNICAL STUDY OF TWO OBSCURE PHOTOGRAPHIC PROCESSES OF THE 19TH CENTURY

I. ABSTRACT

Ruby ambrotypes and sculptographs are two of the more obscure examples of permutations photography has undergone during its first century of existence. Ruby ambrotypes are a variant of the ambrotype, or wet collodion positive, done on a ruby-red 'Bohemia glass' support instead of a clear glass support: a sculptograph is a composite object combining a solar enlargement, a pastel portrait on paper, and a metal bas-relief. Few art historical publications or technical analyses exist for either of these complex processes, though patents, trade catalogues, and photographic manuals of the period describe methods and materials for creating similar objects.

The authors conducted a literature review, visual examination, and scientific analysis to characterize the various organic and inorganic components of both photographic objects in order to determine the probable methods and materials of fabrication. Analytical techniques used include X-ray fluorescence spectroscopy (XRF), ultraviolet/visible (UV/Vis) spectroscopy, Raman spectroscopy, Fourier transform infrared spectroscopy (FTIR), gas chromatography-mass spectrometry (GC-MS), scanning electron microscopy-energy dispersive spectroscopy (SEM-EDS) and backscattered electron imaging. The analytical results will be compared to the materials described in patents and other historic photographic texts, and the impact of these findings on possible conservation treatment protocols will be examined.

II. INTRODUCTION

Photography is constantly evolving but always in pursuit of reality. Since its invention in 1839 it has undergone many permutations, each time a truer likeness was made more quickly and more easily. One technique was invented and another discarded, and in certain circumstances was immediately forgotten.

PART ONE: RUBY AMBROTYPES

1. Introduction

1a. Identification of an Ambrotype

Ambrotypes were popularly produced in America in the decade just before the Civil War. The *common ambrotype* is a wet collodion process produced on a clear glass support. Refer to Figure 1 for a visual interpretation. During exposure of an ambrotype plate in a camera, image highlights receive greater light and become opaque in development. The shadows receive little or no light exposure and are transparent. The image is a negative that when viewed with a black backing appears as positive.

Historically, there were a number of options for preparing the dark backing. One type of backing was coated directly on the glass with a black pigmented Canada balsam or pigmented asphaltum called "black varnish." Sometimes the "black varnish" was applied over the collodion image and viewed through the glass support. Also, backings could be separate from the glass. They were made of black paper, dark velvet or Japanned-tin plates. Figure 2 is a cross section illustration of the common ambrotype. Moor (1976) presents a complete description of variations in the ambrotype presentation.

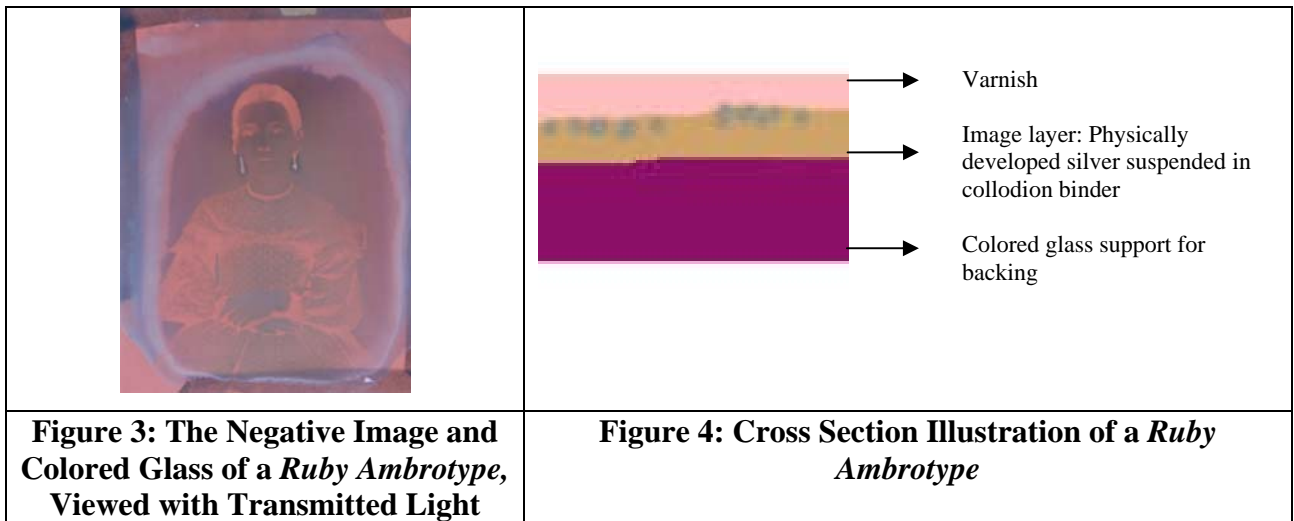| Figure 1: The Common Ambrotype, Plate Half-Removed from Backing to Expose a Negative Image in Transmitted Light	Figure 2: Cross-Section Illustration of a Common Ambrotype

The making of ambrotypes upon a colored glass support started about 1854 in England, and 1856 in America. In reviewing the American published Humphrey's Journal, H.

Draper submitted the earliest entry describing the use of colored glass for ambrotypes on October 1, 1856. The dark glass dually provided a support for the image and a dark backing.

Anthony's Invention and Improvement catalog from 1857 heralded the sale of colored glass by stating, "the colored glass meets a want that has been long felt by Ambrotypists. Made expressly for this purpose at the request of some of the most eminent Ambrotypists."

Today ambrotypes on a colored glass are referred to as *Ruby ambrotypes* or *ambrotypes on Bohemia glass*. When viewing a ruby ambrotype in transmitted light, the colored glass is evident. Most often the color of the glass was reddish to purplish-black in color but there are known samples on green, amber or blue glass. (Osterman, 2007) Figures 3 & 4 elucidate a ruby ambrotype in transmitted light and a cross section illustration.

Varnish

Image layer: Physically developed silver suspended in collodion binder

Colored glass support for backing

Figure 3: The Negative Image and Colored Glass of a *Ruby Ambrotype,* Viewed with Transmitted Light	**Figure 4: Cross Section Illustration of a *Ruby Ambrotype***

1b. Historical Background

The Englishman Frederick Scott Archer introduced the wet plate collodion negative on glass to the photographic societies in the March 1851 issue of the *The Chemist*. One application of Archer's findings was the ambrotype. He described the use of collodion on a glass plate to make a negative of better clarity and quality to the calotype paper

negatives of the day. He did not patent his findings making the technique more available to the public.

The ambrotype was made in sizes similar to the daguerreotype (ninth, sixth, quarter, half, whole plate). They were often housed in cases and bound into packages identical to the daguerreotype. By 1862 and the start of the Civil War in America, the ambrotype process was obsolete. (Newhall, 1958) It had been almost completely replaced by the Ferrotype, a wet collodion process applied to a Japanned iron support. In other parts of the world, the ambrotype enjoyed longer commercial popularity.

1c. Wet Collodion Process and Materials

The binder for the physically developed silver particles in the ambrotype is collodion. Collodion was introduced to the public by the medical profession in 1846 for mending wounds. The term collodion comes from the Greek word meaning *to stick*. It is a less nitrated cellulose nitrate and made when cotton is treated with nitric and sulfuric acid. It degrades, becoming nitrated. Hydroxyl groups and one hydroxymethyl group can be substituted with nitrate groups on the D-glucose in the β-pyranose form. (McGlinchey & Maines, 2005) The fully substituted material is named *gun cotton* and is not soluble in ethers or alcohols. Alternately the less nitrated collodion, also called peroxylin in historic texts, was effectively soluble in ethers and alcohols. Refer to Figure 5 for a structure of collodion.
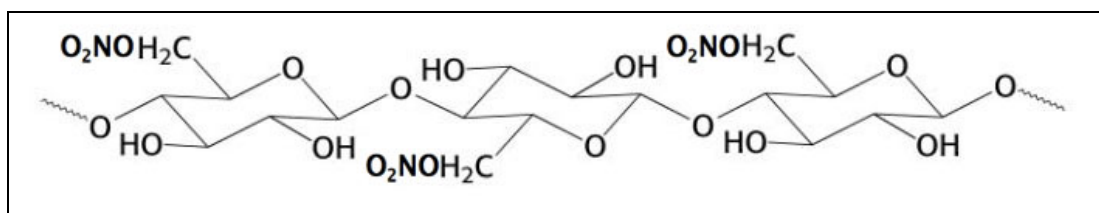

Figure 5: Collodion

The process of coating, sensitizing, exposing, developing, and fixing the ambrotype was done while the collodion binder was wet and known as a *wet plate* method. An ambrotype was made when salted collodion containing iodides and bromides (bromides

were introduced later and allowed the sensitivity into the green region of light), were poured over a polished piece of plate or window glass.
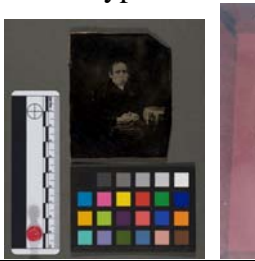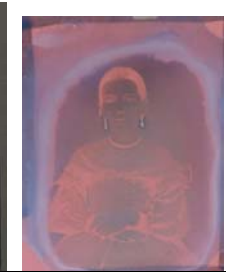
The plate was sensitized in a bath of silver nitrate, and exposed in a camera. Often the image was underexposed to produce a lighter image. They were developed in ferrous sulfate, and fixed in sodium thiosulfate or potassium cyanide. The plate was washed and then often varnished to protect the image from damage during handling.

1d. Coatings Applied to Ambrotypes

Most photographers of the 1850s purchased varnishes ready-made from photographic catalogs. They also made their own, following recipes outlined in treatises of the time and photographic journals. Varnishes were usually natural resins dissolved in alcohols or turpentine but could have easily been polysaccharides, waxes, or proteins. (McCabe et al, 2005)

1e. Colored Glass for Ambrotypes

A photographic text described the colored glass used in ambrotypes as the "finest quality of a medium thick plate glass" (Burgess, 1857), although it is likely that a photographer used whatever materials were available. A lower quality glass called *common glass* or *window glass,* with bubbles and striations, was also used. Most photographers bought their glass pre-cut from photographic warehouses in New York and Philadelphia. In a personal discussion with M. Osterman (2007), he believes that warehouses likely purchased the ambrotype glass from stained window glass manufactures.

Table 1

Reference Number and Image in Reflected and Transmitted Light	Description and Condition
Ambrotype_1	Dimension: 2 ½" x 2" x 1/16" (h x w x d) Ninth plate size portrait of a young man. The glass had an orangish red cast in transmitted light. It was purchased on Ebay in poor condition, as the support and cover glass were broken. There was significant deterioration of the image at the edges and also associated with cracks in the cover glass.
Ambrotype_2	Dimension: 3 ¼" x 2 5/8" x 3/32" (h x w x d) Sixth plate size portrait of an old man from the Winterthur/ UD study collection. The color of the glass was darker than the rest and had a violet cast compared to the orange cast of the others. The image surface was in good condition except for abrasions likely caused by the lack of appropriate housing is storage.
Ambrotype_3	Dimension: 2 ½" x 2" x 3/32" (h x w x d) Ninth plate size portrait of a young woman bought on Ebay. The glass had an orangish red color in transmitted light and there was deterioration of the image at the edges.
Ambrotype_4	Dimension: 2 ½" x 2" x 3/32" (h x w x d) Ninth plate size portrait of a young man from the Winterthur/UD collection. The color of the glass was cranberry color in transmitted light. The silver image was deteriorating at the edges.
Ambrotype_5	Dimension: 3 1/8" x 4" x 3/32" (h x w x d) Quarter plate size portrait of a family purchased on Ebay. The color of the glass was reddish purple in transmitted light. The silver image was in good condition with no visual sign of deterioration.

2. Experimental

2a: Sample Selection

Five ruby ambrotypes were selected for analysis to determine the colorants in the glass support, identify the composition of the varnish and study the tarnish of the silver image. Two of the ambrotypes (Ambrotype_2 and Ambrotype_4) were from the Winterthur/ University of Delaware Program in Art Conservation study collection. The others (Ambrotype_1, Ambrotype_3, and Ambrotype_5) were purchased by the author, bought on Ebay in the past year. Table 1 is a compilation of images and a description of the five ruby ambrotypes.

2b. Methodology

2i. Visual Interpretation with an Ultraviolet Light

Ultra-violet Light Examination. All 5 ambrotypes were removed from their packages and viewed with a UVP Inc. Handheld Shortwave/Longwave UV Lamp, Model UVGL-58. Any fluorescence associated with coatings or varnishes was noted.

2ii. Vibrational Spectroscopy

FT-IR in transmission mode. Each ambrotype was surface cleaned with pressurized air to remove possible contaminants from the surface. Minute representative samples, on the order of micrograms, were removed with a clean scalpel utilizing a Nikon SMZ800 microscope and Sony Trinitron monitor. The samples were placed on a diamond cell and uniformly flattened with a steel roller. The cell was placed on the microscope stage of the Nicolet Magna-IR 560 Esp. Spectrometer and focused. Spectra were collected in transmission mode from samples on all five ambrotypes. Readings were taken for 120 scans between 4000-650 cm^{-1} and a spectral resolution of 4 cm^{-1}. The generated spectra were brought into OMNIC E.S.P. 1a software and compared to a reference library database.

2iii Chromatography

Gas Chromatography-Mass Spectrometry (GC-MS). Coatings from Ambrotype_2 and Ambrotype_5 were prepared for analysis with the gas chromatography-mass

spectrometer, as analysis using IR instruments was not conclusive. Proper sampling was critical as contamination was possible. GC-MS is often used in addition to FT-IR when studying organic components. Analysis was done using a Hewlett Packard HP 6890 Series GC System equipped with a HP 5973 Mass Selective Detector, a HP 7683 Series Injector, and an HP 59864B Ionization Gauge Controller (calibrated for nitrogen).

Minute samples were removed with a sterilized scalpel and rinsed into a small glass vial with ethanol. The ethanol was essential for collection as the collodion binder and coating is only 2-6 microns in thickness (McCormick Goodhart, 1990) and was easily lost otherwise. The sample was evaporated and derivitized using MethPrep II reagent. MethPrep II converts carboxylic acids and esters to the methyl ester derivatives. Analysis was carried out using the RTLMPREP method on the GC-MS and run using a Hewlett-Packard 6890 gas chromatograph equipped with a 5973 mass selective detector and 7683 automatic liquid injector. The sample was then analyzed in the mass spectrometer. The generated spectra were compared to a reference database of materials.

2iv. X-Ray Methods

X-ray fluorescence (XRF). Using XRF was non-destructive and no sample preparation was needed. All five ambrotypes were placed on the stage of the TRACeR III-V portable XRF spectrometer (Figure 6). The spectrometer had the capability for elemental analysis as low as sodium and utilized a rhenium target x-ray source.

Figure 6: Each Ambrotype was Placed on the Stage and Analyzed with the Portable XRF

Spectra were generated from the verso of all five ambrotype support glasses. The collection time was 100 seconds, with a 40kV acceleration voltage and an anode current of 2.4 µA. After collection in PXRF32 Key Master Technologies, Inc version

3.6.11 software, the characteristic K_α and K_β lines as well as certain L_α and L_β lines identified the elements.

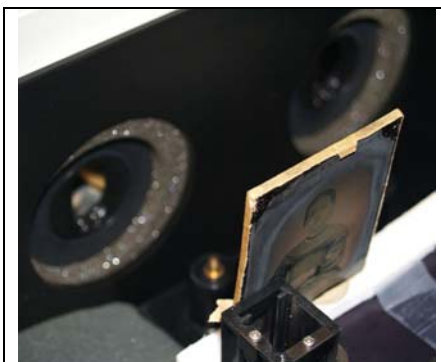### 2v. Ultraviolet and Visible Spectroscopy-Absorbance Mode

Figure 7: An Ambrotype Placed into the Pathway of the Beam During UV/Vis Spectroscopy

The glass was analyzed with a double beam Perkin Elmer Lambda EZ210 Spectrophotometer. A calibration was performed prior to analysis with a holmium oxide standard. Each ambrotype was then surface cleaned on the verso, at one corner, with distilled water. It was placed in the pathway of the sample beam and stabilized on a foam platform and held in place with plastacein putty (Figure 7). The beam passed through areas of glass with no image. Readings were collected between 340-1100 nm with a scan speed of 100 nm/ min. Spectra were plotted by the instrument's proprietary software for absorbance vs. wavelength.

2vi. Electron Beam Methods

Scanning Electron Microscopy-Energy Dispersive Spectroscopy (SEM-EDS). The broken Ambrotype_1 proved to be valuable because it could be studied with the scanning electron microscope. The vacuum chamber on the SEM could hold only up to 3" square and the technique could have been possible without the shattered sample.

A triangular piece from the top right corner was temporarily removed from the object and mounted onto a carbon stub with carbon tape. The sample was heavily tarnished in areas exposed to the environment after the cover glass broke. No further preparation was required. (Figure 8) The triangular piece from Ambrotype_1 was also run in cross-section. It was positioned inside the stub holder and wrapped in copper tape. (Figure 9) In each case, the sample was placed into the chamber and the chamber evacuated.

The SEM functions at magnification of 80X to at least 10,000X, capable of resolving features as small as 0.01 microns. Analysis was performed using a Topcon ABT60 Scanning Electron Microscope equipped with an EDAX 9900 energy-dispersive x-ray analyzer (Philips Electronic Instruments Co.), a cooled SiLi detector, a beryllium window and a tungsten filament gun source. Images were viewed on an Ikegami Monitor.

Black and white backscattered electron images were collected with accelerating voltage of 20 keV and ranging from 500x to 1050x magnification. High incident electron beam with a 20keV accelerating voltage was also used to excite characteristic x-rays from the components of the object. The incident ray penetrates 0.02-1.0 microns into the sample. By using an EDS detector, spot elemental analysis and elemental maps were generated. The EDS detector had the capability of detecting elements in the range of sodium to uranium. All data was collected in Evex NanoAnalysis software.
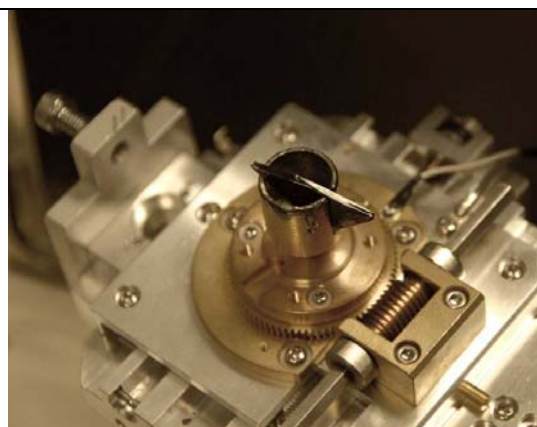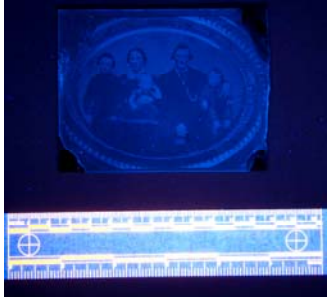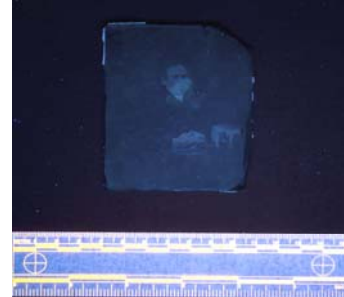

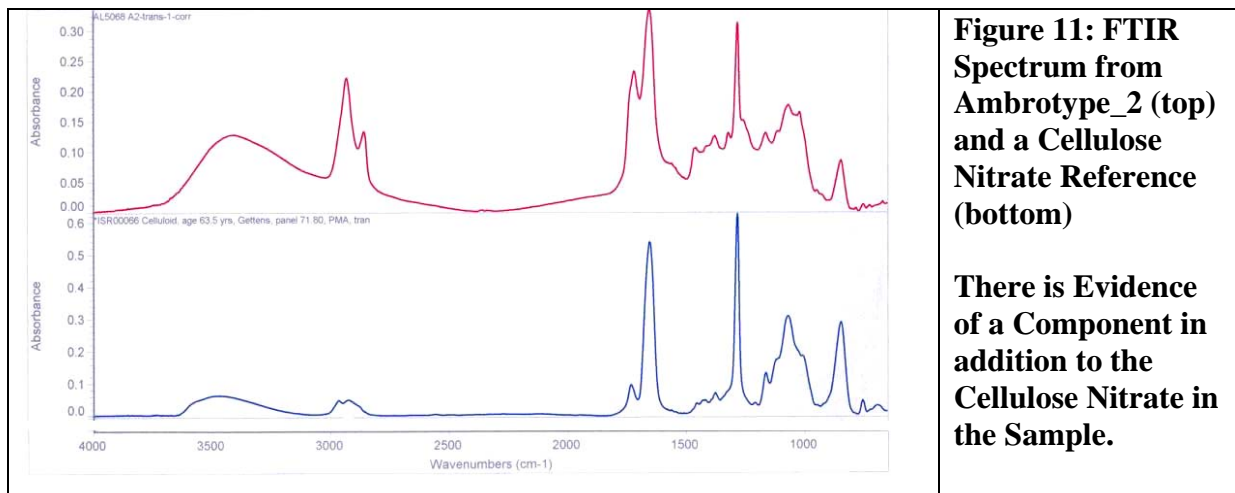| **Figure 8: Sample Mounted for Surface Analysis.** | **Figure 9: Sample Mounted for Cross-Sectional Analysis** |

3. Results

3a. Visual Examination with UV Light

Two ambrotypes of the five fluoresced in long wavelength (366nm) UV light. Three showed no discernable fluorescence, alluding to ambrotypes without a final varnish coating. Figure 10 is images of the fluorescent ambrotypes and a table compiling the data.

		Sample	Fluorescence
a.	b.	Ambrotype_1	none
		Ambrotype_2	yes
		Ambrotype_3	none
		Ambrotype_4	none
Figure 10: Bluish/White Fluorescence of Ambrotype_5 (a) and Ambrotype_2 (b)		Ambrotype_5	yes

3b. Classification of the Coatings with FT-IR

The data collected in transmission mode detected the cellulose nitrate binder in all five samples. On the 3 samples that did not fluoresce in UV light, no other components were detected. In the 2 samples that fluoresced, an additional component was detected. Figure 11 shows that in Ambrotype_2 the peak absorbance at 2900 cm^{-1} is amplified, there is a shoulder off the peak at 1250 cm^{-1} and there is an additional peak at the acidic carbonyl site of 1800 cm^{-1}. The reference library was unable to definitively characterize the additional peaks, but it is very similar to a natural resin.

Figure 11: FTIR Spectrum from Ambrotype_2 (top) and a Cellulose Nitrate Reference (bottom)

There is Evidence of a Component in addition to the Cellulose Nitrate in the Sample.

3c. Characterization of the Coatings with GC-MS

Analysis with the GC-MS revealed a coating with a complex mixture from Ambrotype_2. Ambrotype_5 also had a different but equally complex mixture. Peaks for shellac, sandarac, certain fatty acids and other unidentified high molecular weight resin components were detected in the coating of Ambrotype_2, displayed in Figure 12. The composition of Ambrotype_5 revealed fatty acid components and no resins. There was not enough sample for a full characterization of the coating on Ambrotype_5.

Chromatogram courtesy of Dr. Chris Petersen, Scientific Research and Analysis Lab, Winterthur

Figure 12: The Gas Chromatogram for Ambrotype_2 Revealed a Complex Mixture of Natural Resins and Fatty Acid Components.
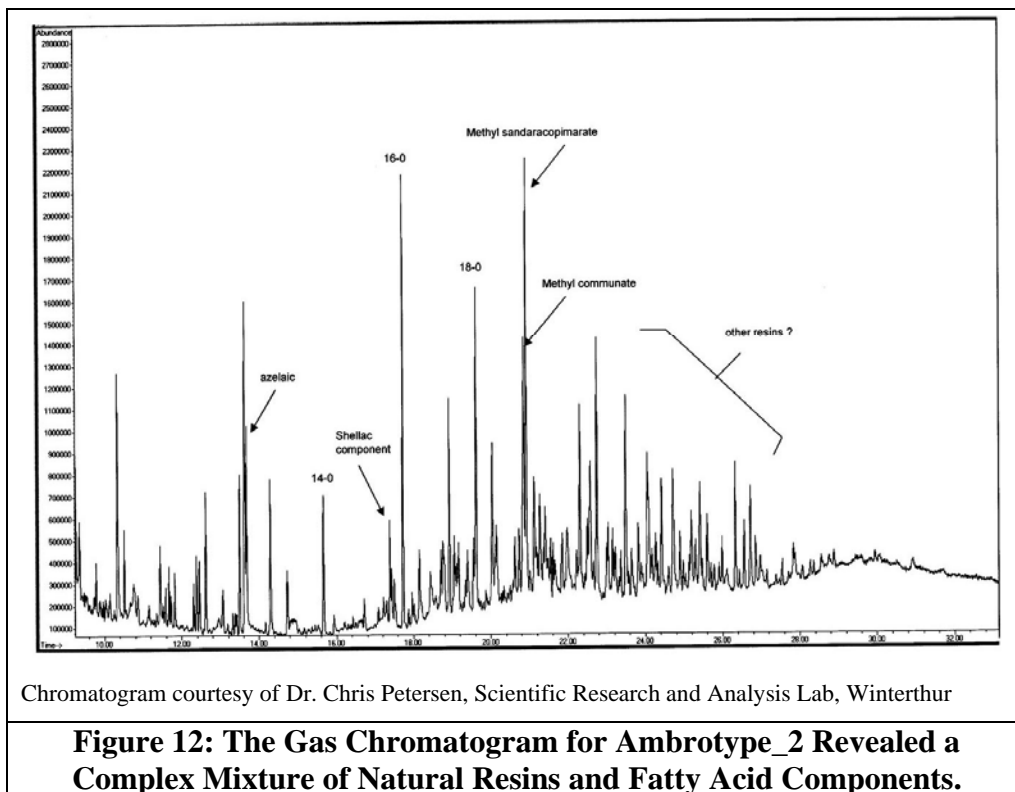
3d. Identification of the Colorants in the Glass Support using XRF

Manganese was identified as the colorant in all five glasses. Four of the glasses also contained additional components of a soda-lime-silica glass matrix. At a scan time of 100 seconds on the portable XRF, one of the lead L_β lines and that arsenic K_α line overlap making conclusive identification of the arsenic peak difficult. In one example, Ambrotype_2, the peak for lead was very strong and distinctive, alluding to a leaded glass matrix. A representative spectrum of a non-lead containing glass from Ambrotype_1 is located in Figure 13. Table 2 is a compilation of the elements detected from each ambrotype using XRF.
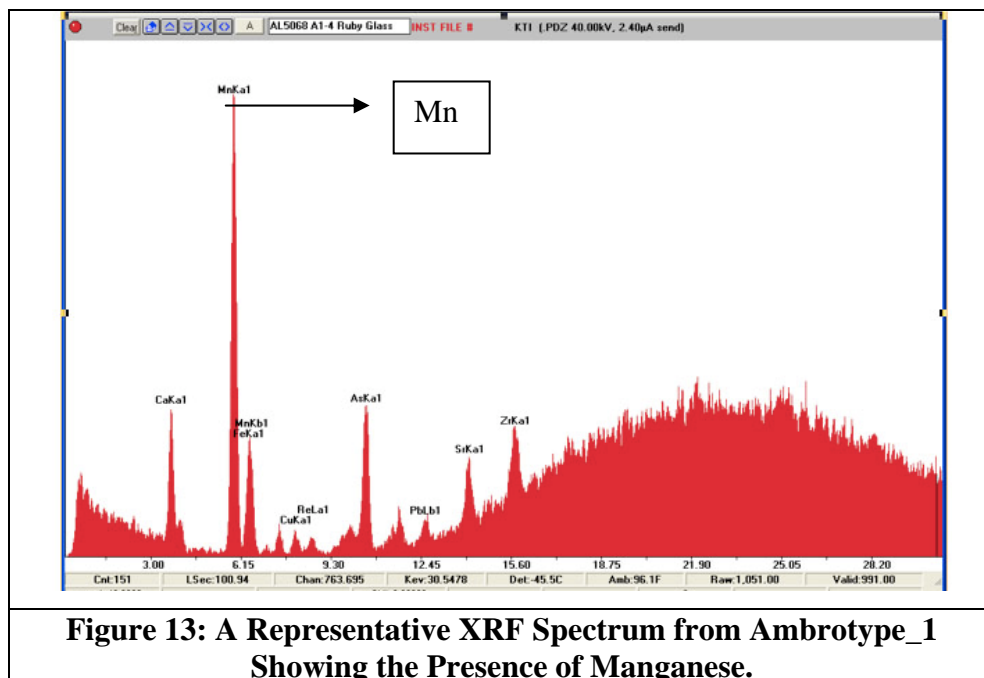
**Figure 13: A Representative XRF Spectrum from Ambrotype_1
Showing the Presence of Manganese.**

Table 2: Data Collected at 100 Seconds with the Portable XRF:							
	Mn	Ca	As	Pb	Fe	Sr	Zr
Ambrotype_1	X	X	inconclusive	inconclusive	X	X	X
Ambrotype_2	X	X	inconclusive	X		X	X
Ambrotype_3	X	X	inconclusive	inconclusive	X	X	X
Ambrotype_4	X	X	inconclusive	inconclusive	X	X	X
Ambrotype_5	X	X	inconclusive	inconclusive	X	X	X

*Ni, Zn and Cu peaks were detected but are artifacts of the filter on the instrument

3e. Absorption Data for Ruby Glass with UV/Vis Spectroscopy

All five ambrotypes generated similar absorption spectra with UV/Vis spectroscopy. They all absorbed light strongly in the visible region of the electromagnetic spectrum, absorbing in the blue/ green and visible as red. There is also a slight absorbance at the shoulder of each spectrum at approximately 650nm. Table 3 shows the maximum peak absorbance for each glass support. Ambrotype_2 was optically more dense than the rest and the absorption exceeded the sensitivity of the instrument. Figure 14 is an overlay of all 5 peaks, showing their similarities. Although Ambrotype_2 was less transparent and did not generate a peak, it appears to closely follow the other curves.
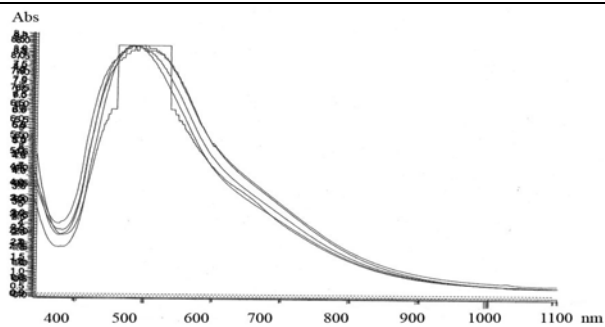
Table 3:	
Sample	Peak Absorbance (nm)
Ambrotype_1	488
Ambrotype_2	exceeded instrument's sensitivity
Ambrotype_3	495
Ambrotype_4	498
Ambrotype_5	506

Figure 14: Absorbance vs. Wavelength (nm) Overlay of the Five Absorbance Spectra.

3f. Surface Analysis with SEM-EDS and BSE

Elemental mapping of the surface was carried out with SEM-EDS in four spots. Spot 4 was taken in cross-section. Figure 15 shows the locations of analysis. Table 4 is compilation of the elements found during analysis.
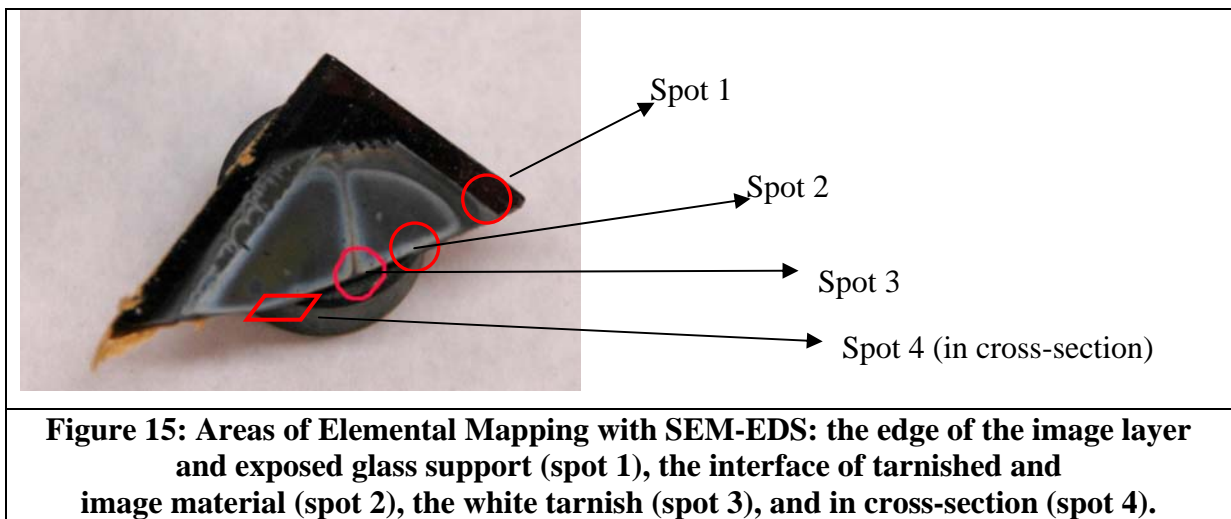
Figure 15: Areas of Elemental Mapping with SEM-EDS: the edge of the image layer and exposed glass support (spot 1), the interface of tarnished and image material (spot 2), the white tarnish (spot 3), and in cross-section (spot 4).

Table 4: Elements detected with SEM-EDS						
	Ag	Cl	S	Ca	Mn	Si
Spot 1	X	X	X	X	X	X
Spot 2	X	X	X	X	X	X
Spot 3	X	X	X	X	X	X
Spot 4	X			X	X	X

Spot 2 revealed a distinct boundary between areas of white tarnish and areas with no white tarnish, seen in Figure 17. Spot 3, a higher magnification of an area of white

tarnish, is shown below with the representative SEM-EDS map. The BSE image from the spot, displayed in Figure 18, revealed large cubic crystals above the background. Elemental mapping located chlorine (yellow), seen in Figure 19, at these crystals. In an overlay of the maps in Figure 20, the crystals also clearly contained silver (red). It is inferred from the data that silver chloride (AgCl) salts stood above a silver sulfide (Ag_2S) background. Sulfur was detected in the background and is evident by light blue pixels. The Ca, Mn and Si were all components from the underlying glass support.

Element	Color
Ag	red
Si	green
Cl	yellow
Ca	pink
Mn	dark blue
S	light blue
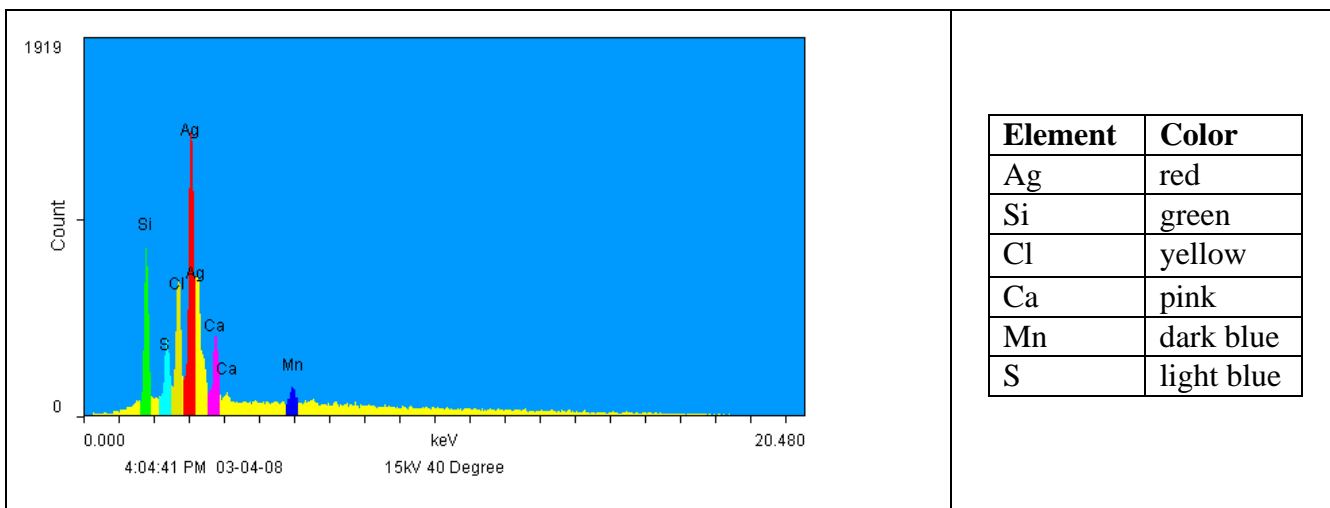
Figure 16: SEM-EDS elemental map and a color chart generated from Spot 3
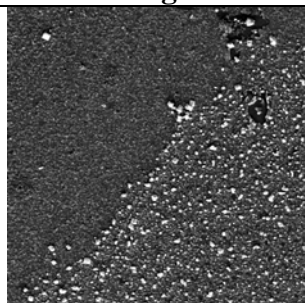
Figure 17: BSE image from Spot 2 showing the distinct line between areas of white tarnish (right) and areas not tarnished (left), 500X

Figure 18: BSE image of surface at Spot 3 in a white tarnished area, 750X

Figure 19: SEM-EDS map from Spot 3 for chlorine (yellow). It is concentrated at the crystals, 750X

Figure 20: SEM-EDS mapping on all six elements. The crystals appear orange because of silver (red) and chlorine (yellow), 750X

4. Discussion

4a. Coatings on Ruby Ambrotypes

Both FTIR and GC-MS revealed evidence for a varnish coating containing natural resin components. Both spectra for the GC-MS revealed a complex and some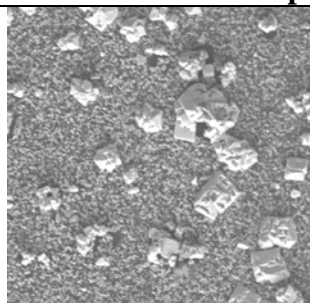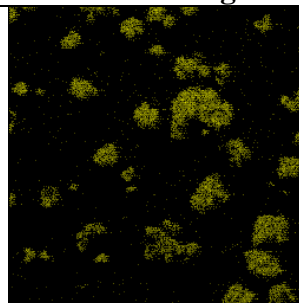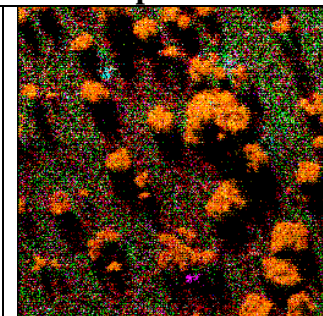what confusing varnish coating. There were peaks from shellac, a common coating used historically, and also peaks coming from components of a sandarac resin, also used historically. However, there is no known mention of using shellac and sandarac in tandem. Both resins are components of spirit varnishes mixable in polar solvents but appear to have been combined with a fatty acid component, possibly a drying oil. Also, certain other unknown resin peaks were noted suggesting the presence of a complex mixture.

It is possible that the coating was an oil resin varnish which has hardened through a polymerization of oils. This was a sandarac resin and linseed oil varnish used into the 19th-century for industry. (Baade, 2008) These coatings were slow cooked under high heat and applied to a surface when cooled. The data are inconclusive since no additional fatty acids characteristic of oils were detected in these tests.

Primary texts were consulted to seek information regarding 19th-century photographic oil resin varnishes. Photographic catalogs sold proprietary ambrotype varnishes, boasting the effectiveness of these secret solutions and revealing nothing of their compositions. (Anthony's catalog, 1857) It is also known that ambrotypists made their own varnishes, following recipes outlined in journals or by word of mouth (Humphrey's Journal, 1857).

Regardless of the ingredients in the varnish, it protected the image from deterioration as the three without coatings show signs of silver tarnish. It was not discovered why ambrotypists did not coat every plate, but it was mentioned they did not like the appearance of a coated image (Burgess, 1858). It appears the aesthetic qualities of the photograph were chosen instead of protecting the image from damage.

4b. Silver Tarnish on Ruby Ambrotypes

When silver is exposed to pollutants and gases in the environment it tarnishes. The mechanism is initiated in an oxidizing environment when an oxide of silver is formed at the surface. In the presence of water, these oxides provide an electrostatic potential that promotes the penetration of corrosive sulfide and chloride ions to attack the structure (Nishimura, 2008).

Figure 21: White Haze Due to the Scattering of Light by Silver Chloride Crystals; Reddish Orange Tarnish is Silver Sulfide Interference Colors

Reducible sulfur is present in the atmosphere from volcanic eruptions as well as generated in combustion reactions. Chlorine components are also prevalent in the environment. They are generated industrially in combustion reactions of plastics, leaded fuels, and coal. It is a common component of particulate matter, especially in areas next to the ocean but also in areas inland.

Photographic image silver is especially vulnerable to attack. Due to the small size of silver grains, there is a large surface area for reactions to occur. Also, the silver particles above the collodion binder are exposed. (McCormick-Goodhart, 1990, 263) In the ambrotype studies it appeared that the scattering of light by small silver chloride crystals caused the whitish haze. The colored tarnish was explained by interference from thin layers of silver sulfide. Figure 21 is a photomicrograph of the tarnish on Ambrotype_1. The presence of sulfides confirms research about tarnish published by others on the surface of cased objects. Image deterioration characterized as chloride crystals is however sparse and warrants additional research. A discussion on the significance of chloride contamination to cased objects is just beginning. Silver chloride salts are sensitive to light and the implications of this deterioration will need to be addressed in the future.

4c. The Colorants for the Ruby Ambrotype Glass Support

Although known as *ruby ambrotypes*, none of the 5 samples were made on a traditional ruby glass. The reddish color was not made with a precipitate of silver or gold, but colored by a complex of manganese in the glass matrix.

A recipe book from 1899 (Biser) provided a number of recipes with manganese in combination with the other metals found using XRF. The recipes for *black glass* best matched the composition. Refer to Appendix 1 for a list of recipes. In reflecting back to an 1857 photographic catalog, the word "purplish-black" glass now seems very appropriate.

Manganese is one of the oldest colorants for glass, dated to as early as 1400 BCE. Chemically, the trivalent manganese (Mn^{3+}) ion produced in a low melt and oxidizing environment, complexes with its surroundings to form a purple glass with a potential to produce a range of colors from reddish to more blue. (Weyl, 1976) The surrounding matrix and concentration are influential in determining the perceived color. The divalent manganese (Mn^{2+}) also plays a role in the color of the glass, although it is much weaker and forms complexes visible in the brown region of the spectrum. (Weyl, 1976).
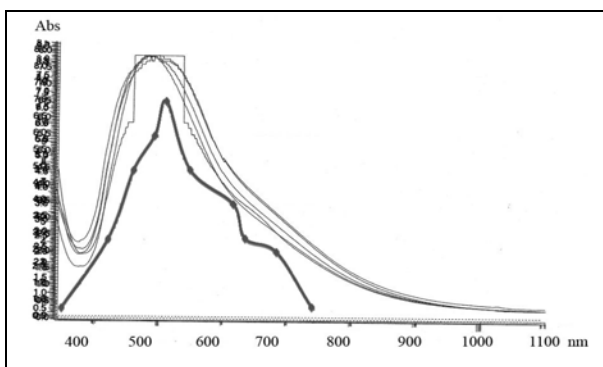
Figure 22: A Resemblance Between the Ruby Ambrotype Spectra and a Reference Spectrum for Glass with Manganese in the Trivalent State.

The peak absorbance of all five ambrotype glasses matched published data for a complex of glass containing trivalent manganese (Mn^{3+}). Green and Hart (1987) studied mid 16th-century glass shards with a UV/Vis spectrometer. Presented were absorption spectra for a red glass containing Mn^{3+} in an octahedral state occurring at λ_{max}=470-520nm. Also, an absorbance

spectrum of trivalent manganese glass was found (Fedotieff, 1924) and overlaid over the five ambrotype spectra from the study, Figure 22. The resemblance is evident and even the small absorbance at the shoulder is present in all the curves.

5. Conclusions

In this small sample of ruby ambrotypes, features not previously discussed in the literature were addressed. The primary colorant in the ruby glass was found to be manganese. The presence of an intact surface coating seems to have protected the image from silver tarnish. When the surface coating was not present, silver tarnish developed in the image over time. The chemical composition of image tarnish found on the ruby ambrotypes was similar to that reported in previous studies of cased-photographic objects. Larger studies of ruby ambrotype images will be necessary to confirm these preliminary findings. The importance of ambrotypes as historical documents of a time period is certain and their preservation is a priority. The implications for conservation treatment and preventive measures are not formed, but are identified as areas of essential study in the future.

PART TWO: SCULPTOGRAPHS

1. Introduction

1a. Introduction to the Object

Of the myriad of permutations photography has undergone in its first century of existence, the sculptograph is surely one of the most unique. A sculptograph combines the qualities of a solar enlargement, a pastel portrait, and a metal bas-relief. The sculptograph discussed in this paper is a portrait of a baby, and belongs to Debbie Hess Norris (AL 5067). See Appendix I for a diagram of the cross section of a typical sculptograph.

The photograph is a solar enlargement of a bald, barefoot baby of indeterminate sex. Extensively re-worked in pastels, few areas of the photograph can be seen by the viewer. The baby's face is the largest of these areas; the pastel was applied to a lesser degree, allowing details of the photograph to be observed. Where the photograph is not completely obscured, the typical characteristics of solar enlargements, soft lines and low image density, are perceptible.

The primary paper support is adhered overall to an unidentified soft, flexible white metal secondary support, possibly lead or aluminum. Intentional deformations of this metal secondary support are what give the sculptograph the appearance of a bas-relief sculpture. The highest point of relief appears to be the baby's nose, which is approximately 3 cm proud of the flat edges of the object. Also in high relief are the head and legs. The flexible metal secondary support is supported by a chipboard backing. The void between the metal and the chipboard backing is filled with a dark red, hard, brittle material, possibly a sealing wax. The framing components, which will not be addressed in this study, include a bronze-painted wooden frame and oval window mat, an unfinished wooden spacer, glazing, multiple nails, and screw eyes and picture wire.

1b. Goals of Analysis

The goal of this analysis was to characterize the various materials comprising a sculptograph and to determine the most likely methods of fabrication. Inorganic

materials such as the photolytic silver constituting the final image of the sculptograph, the metallic secondary support, and the pastel pigments were analyzed using energy dispersive x-ray fluorescence spectroscopy, Fourier transform infrared spectroscopy, Raman spectroscopy, and scanning electron microscopy – energy dispersive spectroscopy. The organic components of the sculptograph were characterized using Fourier transform infrared spectroscopy, Raman spectroscopy, and gas chromatography-mass spectrometry. These constituents included the adhesive used to adhere the paper primary support to the metallic secondary support, the unidentified material between the secondary support and the chipboard backing, and any binder present in the pastels. The fiber composition of the paper primary support was also characterized using polarized light microscopy.

1c. Art Historical Background

No art historical literature or technical analyses was located for these peculiar objects, though multiple methods for various techniques of embossing and creating photographs with bas-relief surfaces were patented. A paper label on the verso of the backing board identifies the object as a *sculptograph* made by the Great Eastern Art Company of New York City. The term *sculptograph* is likely a trade name for the Great Eastern Art Co.'s bas-relief crayon enlargements, though the process used to create them is likely very similar to other photographic firms' techniques. The Great Eastern Art Co., according to the label on the verso of the object, is the "Originators [*sic*] of the bas-relief in portraiture and the only concern making the genuine celebrated raised enlargements on Aluminum Metal." The paper label states that the Great Eastern Art Co. has a "patent

Figure 1: Label on the Verso of the Representative Sculptograph

pending", though whether this was a patent application for the specific process used by the company or for the term *sculptograph* is unknown, as a search of the U.S. Patent Records failed to give any results for either the term or the company.

Two sculptographs recently came up for auction, at Flomaton Antique Auctions (2007) in

Figure 2. Label on the Verso of the "Lady on Sculptured Lead," courtesy of Flomaton Antique Auctions

Eufaula, AL and at Mastro Auctions in Burr Ridge, IL. The photograph offered by Flomaton Antique Auctions is described as a "painting of a lady on sculptured lead". Misidentified as a painting, the object appears to be a pastel- or crayon-embellished solar enlargement. Clearly visible in a detail photograph of the object's verso is a label identifying the object as a sculptograph from the Great Eastern Art Company.

The sculptograph offered by Mastro Auctions (2005) is described as a salt print sculptograph of an 1870's football player. The description of the object continues:

> Interestingly, the undulation, which seems to distort the image, was purposely done so as to provide a three-dimensional 'embossed' effect. When viewed from the sides, portions of the print appear raised.

This sculptograph also has a label stating that it was produced by the same Great Eastern Art Company. Finding the term *sculptograph* in conjunction with that of the Great Eastern Art Company on three bas-relief photographs supports the conjecture that *sculptograph* was the Great Eastern Art Co.'s trade name for such objects.

Multiple patents do exist which describe the materials and methods of creating bas-relief photographs, materials and methods most likely very similar or identical to those used in creating sculptographs. Richard H. Chinn and John L. McGee were awarded a patent for an 'Improvement in Photographic Pictures' in 1874. In 1898, two patents were awarded to Duran F. Hulbert, one for a 'Relief-Photograph and Method of Producing the Same' and the other for 'Embossing Photographs' (1898a, b). Hulbert's (1898a) first patent describes his method of creating a relief photograph:

> Which consists of attaching the photographic print or picture to a pliable, non-elastic, malleable, metallic mount, such as lead, and embossing the mount and print, or picture, and filling the depressions upon the back of said malleable, metallic mount with a plastic material which will harden when cold or dry.

Hulbert's (1898a) second patent, dated to the same day as his first, is more extensive and states that his invention is applicable to "all other kinds of embossed or bas-relief work, as well as to photographs or sun-prints". He uses two mounts, the malleable metallic mount mentioned previously and a cardboard-like material that can be wet and pressed into place and will retain that shape when dry. The metallic mount, "a plate of pliable non-elastic yielding permanently-configurable dry-bodied material, such as sheet lead, an alloy of lead and tin, or the like", is preferred for hand-embossing and a "reinforcing-sheet of paper, thin cardboard, of the like, may be used to great advantage" by being "placed upon the opposite side of the mount from the print".

As to aesthetics, Hulbert (1898a, b) states that "embossed photographs should not be glossy or shiny, and such paper should be used as will avoid this objection". Gelatin or collodion emulsion papers are offensive when used for embossed photographs – the emulsion is glossy and, according to Hulbert, detracts from the beauty of the bas-relief surface. He avoids these faults "by using paper having a rough uncalendered surface and sensitized with a solution of silver nitrate dissolved in water". He also places a sheet of "fine bolting cloth against the face of the print" during the embossing process to help

decrease the surface gloss. See Appendix II for the figures from Hulbert's two 1898 patents which describe the process of making bas-relief photographs.

1d. Related Analytical Work

Though no art historical or scientific literature directly relating sculptographs has been found, the many components of a sculptograph have long been studied by conservators, scientists, and art historians.

X-ray fluorescence spectroscopy (XRF) has been used with some success to gain greater understanding of various image-forming metallic compounds within photographic papers and emulsions (Enyeart et al. 1983; McCabe and Glinsman 1995). Instrumental analysis using Raman spectroscopy has been repeatedly used to successfully identify the compounds/phases present in a sample. Fourier transform infrared spectroscopy (FTIR) is frequently used to characterize the general functional groups present within natural or synthetic organic components of objects. It is highly effective, providing good spectra even with very small amounts of sample (Low and Baer 1977). It can also be used to carry out phase identification of certain inorganic compounds, an attribute often exploited in pigment analysis. In a similar vein, gas chromatography-mass spectrometry (GC-MS) is frequently used for analysis of organic components.

2. Experimental Procedures: Analytical Instruments and Sampling Procedures

2a. Polarized Light Microscopy

Nikon Eclipse E600 POL Polarizing Light Microscope
    (10, 20, 40x objectives)
    Diagnostic Instruments SPOT RT Digital Camera with accompanying software
Graff's C-Stain, manufactured by Integrated Paper Services, Inc.

Samples were taken using a fine needle tool, lightly dampening the area to be sampled and carefully removing fibers from the paper. The fibers were placed into a clean glass slide and teased apart, cover slipped, wetted with deionized water, and examined. The samples were then stained with Graff's C-Stain and examined a second time.

2b. X-Ray Fluorescence Spectroscopy

ArtTAX Micro-XFR Spectrometer

      Molybdenum x-ray tube source, 100-300 seconds collection time
      300-600 microamps range, polycapillary X-ray lens
      Collected and interpreted with ArtTAX Ctrl (RONTEC GmbH) 3.5.0.20 Software

Bruker Portable XFR Spectrometer
      Rhenium tube source
      100-300 seconds collection time
      2.4-15.0 microamp range, 15-40 kV range

As the instrumental technique is non-destructive and both pieces of equipment are open-architecture design, no sampling was required. See Appendix III for analysis locations.

2c. Raman Spectroscopy

Renishaw InVia Raman Microscope
      3 cm^{-1} spectral resolution
      Diode lasers, 514 and 785 nm excitation sources
      Diffraction grating is 1200 lines/mm
      Collected and obtained using Wire 2.0 Software

Samples ranging between μgs and mg were taken by lightly scraping a clean scalpel blade across the surface and were stored between two glass microscope slides. The samples remained on the glass slides for analysis. The University College of London Raman Spectroscopic Library (accessed 2/1/2008) and Burgio and Clark's article (2001) were used for reference spectra. See Appendix III for sample locations.

2d. Fourier Transform Infrared Spectroscopy

Nicolet Magna Infrared 560 Spectrometer
      Used in conjunction with a Nic-Plan IR Microscope
      4 cm^{-1} resolution, 4000-650cm^{-1} range, 120 scans
      Spectra interpreted with Nicolet 7.2 OMNIC software

The same samples analyzed using the Raman spectrometer were also analyzed using the FTIR spectrometer. Samples were transferred to a clean diamond cell and were flattened in preparation for analysis. Various IRUG and commercial reference spectral libraries were searched using the software for the best-fit matches. See Appendix III for sample locations.

2e. Gas Chromatography-Mass Spectrometry

Hewlett Packard HP 6890 Series GC System
      HP 5973 Mass Selective Detector
      HP 7683 Series Injector

HP 59864B Ionization Gauge Controller

This was done after FTIR analysis to determine the preliminary functional groups present within the sample, enabling the selection of the appropriate derivation method. An oleo-resinous sample taken for FTIR and Raman analysis was used for GC-MS analysis. The sample was prepared using the commercial derivation procedure, MethPrep 2.

2f. Scanning Electron Microscopy: Electron Dispersive Spectrometry and Backscattered Electron Imaging

Topcon ABT Scanning Electron Microscope
Gold reference calibration standard
EDAX 9900 detector (EDS), Philips Electronic Instruments Co.
Ikegami Monitor

Samples were obtained by collecting loose fragments of the materials to be analyzed. The samples were adhered to a carbon stub and placed into the SEM-EDS chamber for analysis.

3. Results

3a. Polarized Light Microscopy

A sample of the paper primary support was taken from the lower center edge, in an area of existing damage. Examined visually, the majority of the fibers appeared to be bast fibers, as nodes in the fibers were observed both in transmitted and polarized light. Upon staining with Graff's C-stain, the majority of the fibers stained a purple-yellow. This is indicative of a paper containing a majority of bast fibers.

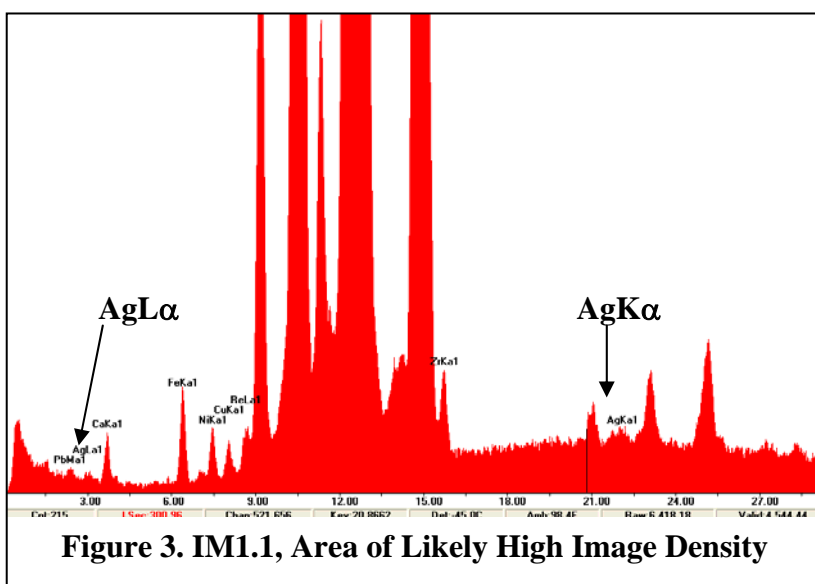### 3b. X-Ray Fluorescence Spectroscopy

X-ray fluorescence spectroscopy was used to analyze the elemental compositions of the sculptograph's inorganic components,

Figure 3. IM1.1, Area of Likely High Image Density

such as the secondary support, image-forming silver, red fill material, and pastel pigments.

As most of the solar enlargement is covered with pastel, the areas of high image density that would have the most silver are hidden beneath pigments. In an attempt to detect the photolytic silver making up the final image, several spectra were gathered in areas of likely high image density. Figure 3 is an example of the x-ray fluorescence spectra collected in such an area indicating the presence of silver. The level of confidence is high, as the doublets of both the silver Lα and Kα lines are present.

Figure 4 is an XRF spectrum typical of the metallic secondary support. The overwhelming element present is lead. Aluminum was not detected in any XRF analysis, not even when the instrument detector's filter was
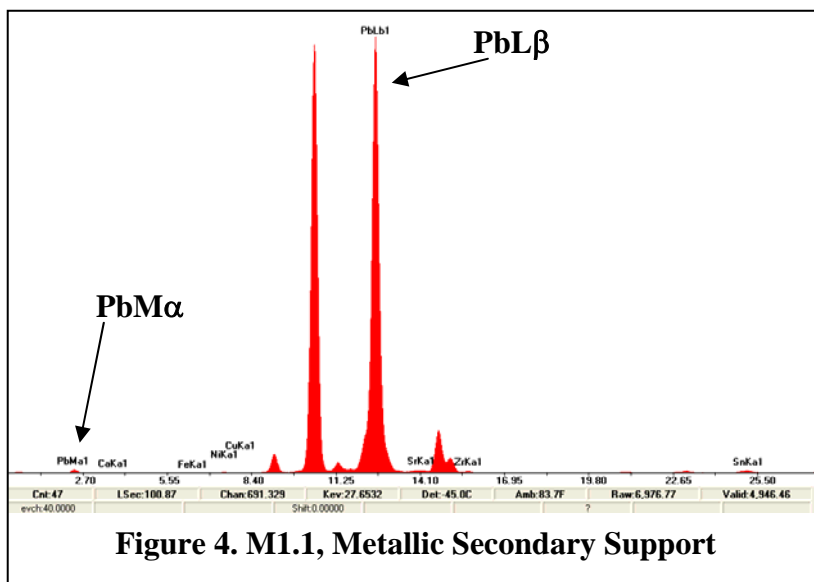

Figure 4. M1.1, Metallic Secondary Support

removed in order to permit the detection of lower molecular weight elements. Table 1 summarizes the XRF data gathered from the inorganic components of the sculptograph and lists components inferred based upon the elements present.

Table 1. Summary of X-Ray Fluorescence Data

Site	Major Elements	Minor Elements	Time	Components Inferred
Metallic Secondary Support				
M1.1	Pb†	Ca, Fe, Cu‡, Ni‡	100 s	Lead
M1.2*	Pb	Ca, Fe, Cu	100 s	Lead

Red Fill Material				
F1.1*	Ca, Ba, Fe	S, Ar§, Ba, Cu	100 s	Iron oxides
				Gypsum
				Calcium carbonate
F1.2	Ca, Ba, Fe, Sr	Ar, Ni, Cu, Sn	100 s	Iron oxides
				Gypsum
				Calcium carbonate
Areas of Potential High Image Density				
IM1.1	Ca, Pb, Zn	Ag, Fe, Ni, Cu	300 s	Photolytic silver
				Chalks
IM2.1	Ca, Mn, Fe, Pb	Ag, Ni, Cu, Zn‡	300 s	Photolytic silver
				Iron oxides
				Umber
				Chalks
IM3.1	Ca, Fe, Pb	Ag Ni, Cu, Zn	300 s	Photolytic silver
				Iron oxides
				Chalks
Applied Pastels				
P1.1, blue	Pb	Ca, Fe, Ni, Cu	100 s	Chalks
P2.1, green	Fe, Pb	Ca, Ba, Cr, Ni, Cu, Zn	100 s	Iron oxides and/or Prussian blue
				Chrome yellow
				Fillers: chalks, barite
P3.1, white	Ca, Pb	Fe, Ni, Cu, Zn	100 s	Chalks
P4.1, pink	Pb	Ca, Fe, Ni, Cu, Zn	100 s	Chalks
P5.1, flesh	Ca, Fe, Pb	Ni, Cu, Zn	100 s	Iron oxides
				Chalks
P6.1, light grey	Ca, Pb	Fe, Ni, Cu, Zn	100 s	Iron oxides and/or Prussian blue
				Chalks
P7.1, dark grey	Ca, Ba, Fe, Pb	Ni, Cu, Zn	100 s	Iron oxides and/or Prussian blue
				Chalks

* The detector's filter was removed in order to distinguish lower atomic weight elements. For these spectra, the analysis parameters were changed to 15 kV and 15.0 µA. Unless noted, all other spectra were acquired using 40 kV and 2.40 µA.

† Lead produced a large signal in each XRF analysis excepting the red filler material because the filler material was removed from the body of the sculptograph before analysis: the large amount of lead also caused two photon peaks to occur throughout each spectrum.

‡ Copper, nickel, and zinc, which occur throughout XRF analysis had very small peak heights, are common components of surface dirt and are probably not present within the metal secondary support or applied pastels.

§ Argon gas was identified when the filter was removed.

3c. Fourier Transform Infrared Spectroscopy

Table 2. Summary of Fourier Transform Infrared Spectroscopy Data

Site	Matches
Red Fill Material	
F1.1, clear matrix surrounding particles	Pine resin
	Barite and/or lithopone
F1.2, mix of solid particles and clear matrix	Pine resin
	Chalks

Adhesive	
A1.1, scraping of pooled adhesive	Almond gum Cellulose
Applied Pastels	
P1.1, white	Gypsum Almond gum
P1.2, white	Gypsum Almond gum
P2.1, dark green	Prussian blue Almond gum
P2.2, dark green	Prussian blue Almond gum Calcium carbonate
P4.1, black	Bone ash Calcium carbonate Gum?
P5.1, flesh tone	Gypsum Calcium carbonate
P5.2, flesh tone	Gypsum Calcium carbonate

Fourier-transform infrared spectroscopy was used in two ways: to carry out preliminary organic analysis and to provide compound/phase identification of some inorganic materials. The table above, Table 2, is a summary of the FTIR data gathered from these various components.

Figure 5. F1.1, Red Fill Material

This preliminary FTIR analysis indicated that a major component of the filler material was likely pine resin. As seen in Figure 5, the unknown (red) is a strong match for the pine resin reference sample (purple).
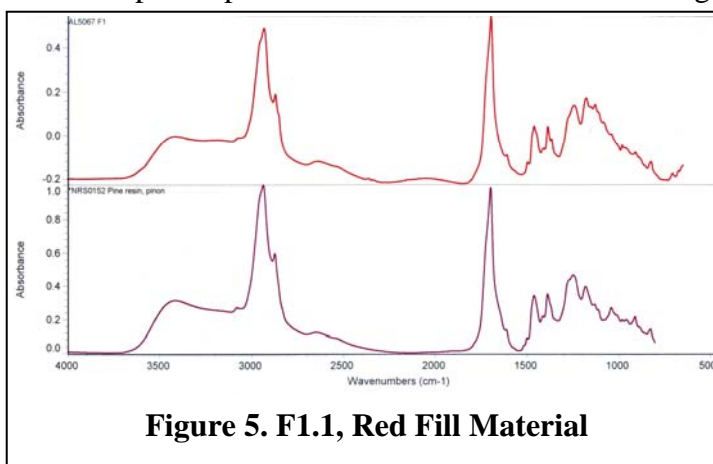
3d. Raman Spectroscopy

Raman spectroscopy was used to identify the inorganic compounds present within the red filler material and applied pastels. The compound/phase analysis possible with Raman

served two purposes: to identify materials that FTIR is not capable of detecting and to reinforce identifications made using the FTIR spectra.

Table 3 is a summary of the Raman spectra collected. The pigments detected were identified based upon the matches of peaks characteristic to certain materials. Two different laser excitation sources were used, a 514.5 nm wavelength laser and a 785 nm wavelength laser.

Table 3. Summary of Raman Spectroscopy Data

Site	Source λ	Identification (indicative peaks, cm^{-1})
Red Fill Material		
F2.1, red particle	785 nm	Red Ochre (220, 286, 402, 491, 601) Gypsum (415, 1009, 1136)
F2.2, clear particle	785 nm	Red Ochre (220, 286, 402, 491, 601) Gypsum (1009, 1136)
Applied Pastels		
P1.1, white, representative particle	514.5 nm	Gypsum (415, 1009, 1136)
P2.1, dark green, dark particle	514.5 nm	Carbon black (~1325, ~1580)
P2.4, dark green, red particle	514.5 nm	Prussian blue (2102, 2154) Chrome yellow (361, 842) Carbon black (~1325, ~1580)
P3.1, light grey, blue particle	785 nm	Lapis lazuli* (258, 548, 1096) Calcium carbonate (283, 1087)
P3.1, light grey, yellow/red particle	785 nm	Iron oxide (220, 286, 402, 601) Calcium carbonate (283, 1087)
P3.1, light grey, black particle	785 nm	Carbon black (~1325, ~1580)
P3.1, light grey, clear particle	785 nm	Calcium carbonate (1087)
P4.2, dark grey, blue particle	785 nm	Lapis lazuli (548, 1096)
P5.1, flesh tone, red particle	785 nm	Vermillion (253, 284, 343)
P5.3, flesh tone, blue particle	514.5 nm	Lapis lazuli (258, 548, 822, 1096)
P5.4, flesh tone, clear particle	514.5 nm	Gypsum (179, 415, 493, 619, 670, 1009, 1136)
P6.1, black, black particle	514.5 nm	Carbon black (~1325, ~1580)
P6.2, black, clear particle	514.5 nm	Carbon black (~1325, ~1580) Barium sulfate (553, 988)

* Lapis lazuli may also be known as ultramarine blue.

As seen in Table 3, the majority of the pigments detected were iron oxides and chalks such as calcium carbonate and calcium sulfate (gypsum). Several other, slightly more unusual, pigments were detected. These include vermillion (Fig. 6), lapis lazuli (Fig. 7), Prussian blue (Fig. 8), and chrome yellow (Fig. 8).

XRF analysis of the filler material (Table 1) suggested that an iron oxide was likely present. Because FTIR spectroscopy is not capable of detecting iron oxides and Raman spectroscopy is, Raman analysis was used to examine the filler material. Raman identified the dark red particles within the filler material as an iron oxide, likely a red earth pigment,
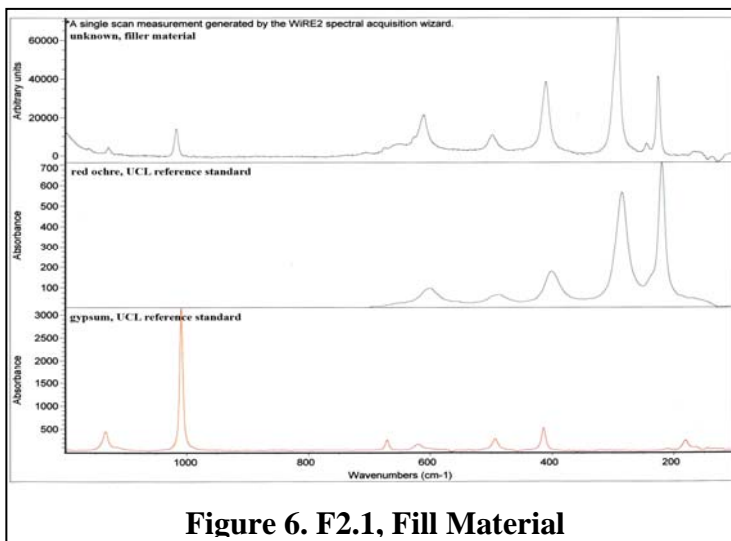

Figure 6. F2.1, Fill Material

and gypsum, a pigment that is also utilized as an extender. As seen in Figure 6, the reference samples of red ochre (green) and gypsum (red) are good matches for the peaks present within the Raman spectra of the unknown sample (blue).
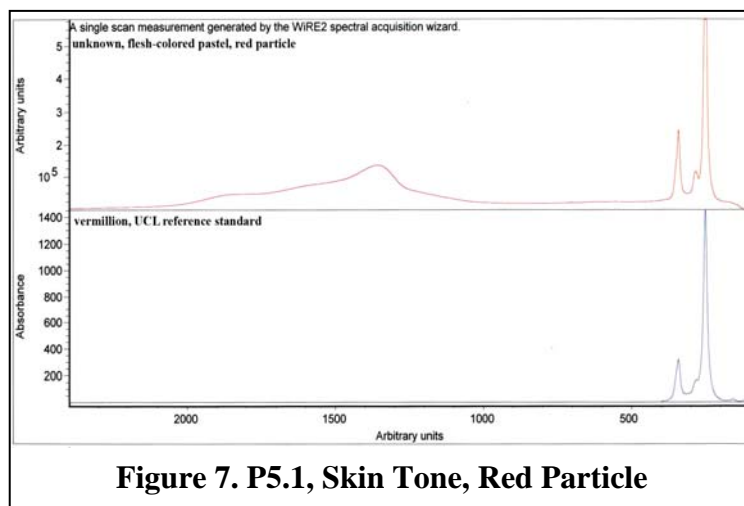

Figure 7. P5.1, Skin Tone, Red Particle

As mentioned previously, Figure 7 is an example of one of the more usual pigments detected. Pictured below (Fig. 7), the reference sample of vermillion (blue) is a good match for the unknown sample (red). The presence of vermillion was not detected using any other analytical techniques, perhaps because a small amount was used. Larger quantities of vermillion can be detected using XRF: identification of mercury is usually indicative of the presence of vermillion pigment, a mercuric sulfide (Gettens and Stout 1942).

Figure 8 is an example of the spectra acquired from a pigment particle containing lapis

Figure 8. P5.3, Skin Tone, Blue Particle
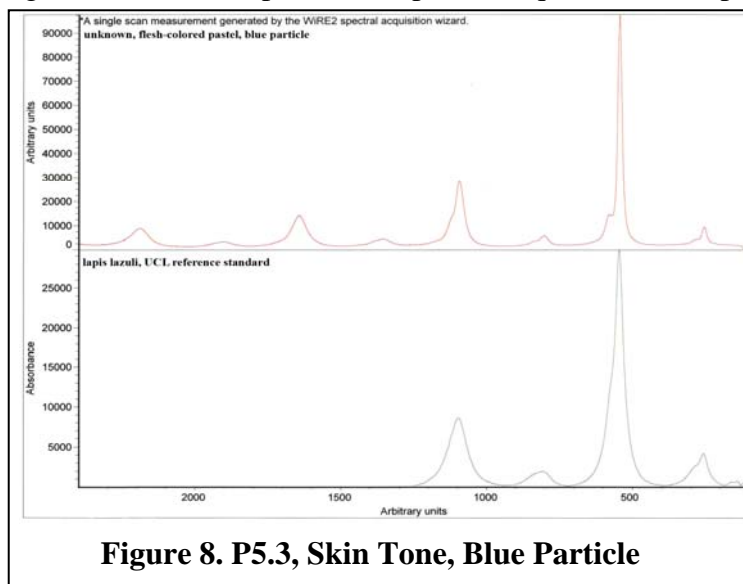
lazuli, the semi-precious stone used to make the pigment ultramarine blue (Gettens and Stout 1942). Lapis lazuli's characteristic signal is due to the lattice-wide vibrations of the crystals within the pigments. As seen in Table 3, multiple samples contained lapis lazuli.
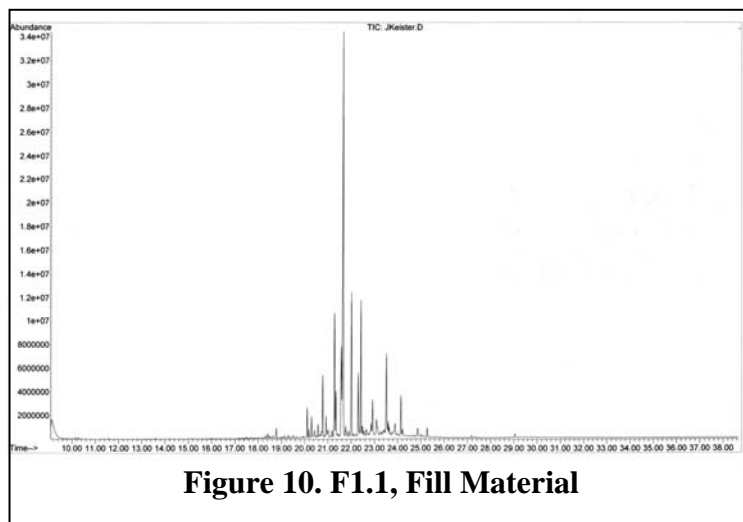
Figure 9 is the spectra of a sample taken from the large field of dark green pastel. The unknown sample (blue) contains the characteristic peaks of Prussian blue (red), chrome yellow (green), and a carbonaceous black (orange). Prussian blue was identified previously using FTIR analysis (Table 2), as the nitrile groups in Prussian blue give characteristic peaks when analyzed using FTIR. The results of the Raman analysis serve to confirm this identification.

Figure 9. P2.4, Dark Green Pastel, Red Particle
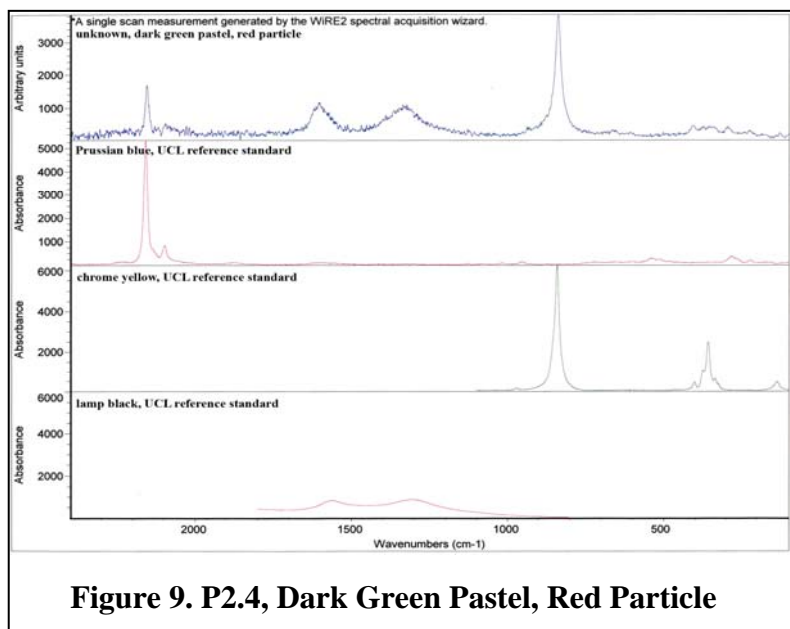
Chrome was identified in XRF analysis of the dark green pastel, indicating that chrome yellow may be present. The identification of chrome yellow in the samples was confirmed via Raman spectroscopy.

3e. Gas Chromatography-Mass Spectrometry

A sample of the fill material was submitted for gas chromatography-mass spectrometry in order to confirm the identification of the resinous component of the filler. GC-MS analysis confirmed the identification as pine resin, as the sample's chromatograph was characteristic of a pine resin, abet a pine resin that was not highly oxidized.

Figure 10. F1.1, Fill Material

3f. Scanning Electron Microscopy: Electron Dispersive Spectrometry

A sample of the metallic secondary support was analyzed using the scanning electron microscope. This was done because low molecular weight elements such as aluminum

are difficult to detect in open-air XRF systems. As seen in the elemental spot analysis and maps, aluminum was not present in any significant amount. Other minor elements are likely due to surface dirt and paper fillers. A small amount of aluminum was detected however, small amounts of aluminum found in conjunction with silicon is often indicative of an alumino-silicate, a common contaminant of mined materials such as iron oxides.

Figure 11. M1.1, Metallic Secondary Support, 420X
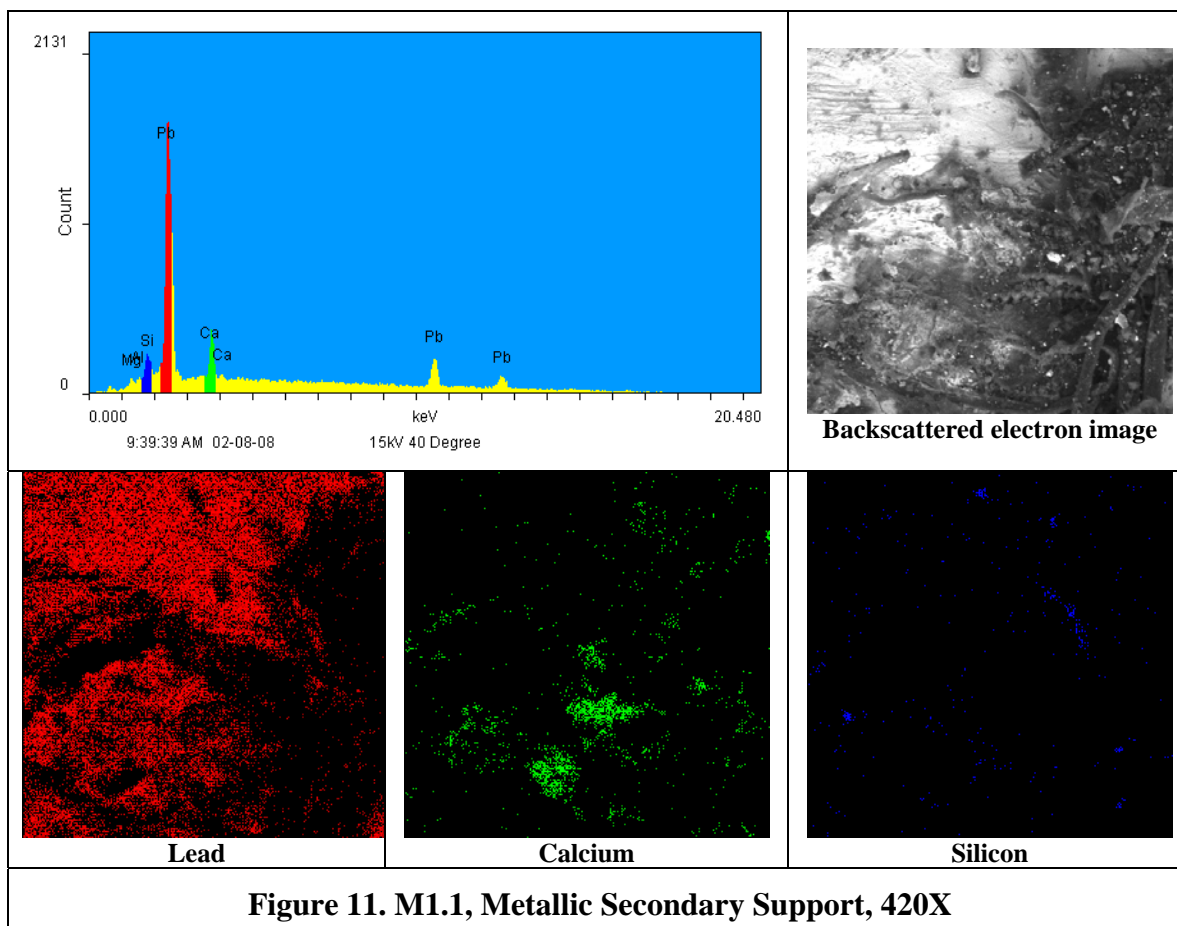
A sample of the filler material was also examined using the scanning electron microscope (Fig. 12). The elements present, such as iron, sulfur, calcium, and barium correspond to the compounds detected using FTIR and Raman spectroscopy. In the elemental map, all

of the elements identified appear clustered together in small clumps. This is expected for a material that is a mixture of inorganic pigments suspended in an organic binder.
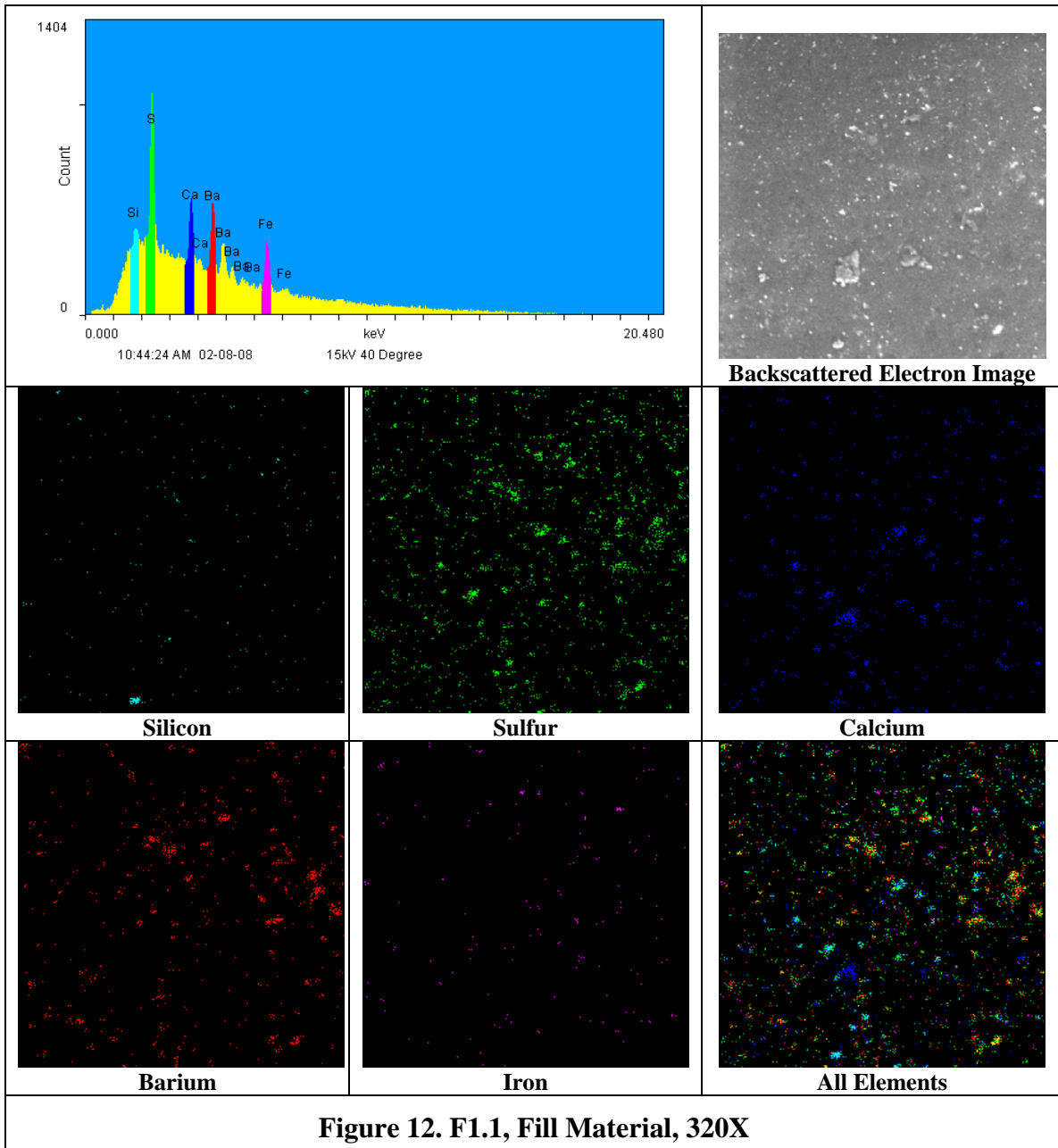

Figure 12. F1.1, Fill Material, 320X

4. Discussion

4a. The Photographic Image

Solar enlargements, also known as crayon portraits or enlargements, were created using copy negatives of previously existing photographic originals. Methods of enlarging photographs were developed and patented as early as 1843, and by 1856 the solar cameras used to create enlargements were commonplace. The final photographic image produce was of low density and in order to 'strengthen' it a variety of materials were applied: ink, watercolor, gauche, charcoal, crayon, pastels, or airbrushes (Albright and Lee 1989).

The characteristic low image density of a solar enlargement was evident within the sculptograph analyzed. This is unsurprising, as it is evident through a visual examination of the object and perusal of historic texts that the photographic component of a sculptograph is a solar enlargement. X-ray fluorescence was used to detect the silver image-forming material within the solar enlargement, the photographic component of the sculptograph. Attempts were made to carry out the analysis in areas of high image density, as these areas would contain the most silver metal. This type of analysis is can be difficult to carry out on photographic processes containing more image material than solar enlargements (McCabe and Glinsman 1995). Also, as the applied pastel obscures most of the solar enlargement, guesses as to the location of the areas of high image density were made based upon the imagery of the baby. Silver was identified in several of these areas (Fig. 3). In most cases, the doublets of both the silver Lα and Kα lines were detected.

4b. The Primary Support

The primary paper support appears to consist of middle-to good quality bast fibers. Good quality papers were necessary for the successful creation of a photographic print. The adhesive attaching the solar enlargement to the metallic secondary support was identified as a gum-based adhesive using FTIR spectroscopy. This is consistent with adhesives used in the late 19th and early 20th centuries.

4c. Pigments Used to Embellish the Sculptograph

Analysis by XRF, FTIR, and Raman spectroscopy identified the pigments present within the pastels used to embellish the photograph. The pastels all appeared to utilize a gum binder: the exact identities of the gums used may vary, but for the purpose of this analysis any such variance was not significant (Table 2). The pigments identified are typical of the estimated date of the object, the last quarter of the 19th century. They include gypsum, calcium carbonate, barium sulfate, chrome yellow, Prussian blue, ultramarine blue, vermillion, and multiple iron oxide pigments (Tables 1-3 and Figs. 7-9). Historically high-priced pigments such as ultramarine and vermillion were available as synthetic pigments during this time, so their inclusion is not surprising (Gettens and Stout 1942).

A limited number of samples were taken (Appendix 3): areas such as the face, lips, and eyes of the baby were not sampled. The similarity of colors between the unsampled baby's face and lips and the sampled heel of the foot suggest that vermillion was also utilized in these areas.

Two blues pigments were used to color the sculptograph, Prussian blue and ultramarine blue (Fig. 8 and Fig. 9). Either pigment, or a mixture or both, could have been used to tint the eyes. As Prussian blue was only found as a component of a green colored area and the ultramarine blue found throughout the sculptograph, it is likely that the pigment used to color the eyes was ultramarine. The color of the eyes also suggests the use of ultramarine blue. As seen in Table 1, no elements indicative of either Prussian blue or ultramarine blue were detected. However, as ultramarine blue is an alumino-silicate consisting mainly of lower molecular weight elements, it would be more difficult to detect in an open-air XRF system and may be present but undetected.

The dark green pastel (Fig. 9) containing chrome yellow, Prussian blue, and carbon black was likely mixed prior to application to the photograph. This is because the edges, which are ordinarily hidden beneath the framing elements, are smeared with pastel of the same even dark green tonality of the exhibited dark green color field.

4d. The Red Filler Material

The filler material is a mixture of an organic binder and various inorganic pigments. In the elemental maps pictured in Figure 12, all of the elements identified appear clustered together in small irregular clumps. This is expected for a material such as the filler, which is a mixture of inorganic pigments suspended in an organic matrix.

The filler's organic binder was first characterized as a pine resin through FTIR spectroscopy (Fig. 5): this was confirmed via GC-MS (Fig. 10). As stated previously, the pine resin is not as highly oxidized as would be expected in a pine resin dating to the later half of the 19th century. However, this lack of oxidation is not surprising as the thickness of the filler and its location between the backing board and the metallic secondary support would have protected it from oxygen exposure. Pine resin would be an appropriate selection as a filler material, as it fulfills the requirements stated for a fill material by patents contemporaneous with the object as being "a plastic material which will harden when cold or dry," (Hulbert 1898a).

As stated previously, analysis using XRF, FTIR, and Raman spectroscopy identify the main inorganic components within the filler as iron oxide and gypsum (Fig. 6) and the minor inorganic components as calcium carbonate and barium sulfate. These results are further confirmed by the SEM-EDS analysis of a fragment of the filler material (Fig. 12). The elements detected include sulfur, calcium, barium, iron, and silicon. They correspond to the pigments detected using the other analytical methods: silicon is likely present as an extender or contaminant. The iron oxide serves to pigment the resin while the other inorganic components act as colorless fillers. The fillers may have been added to thicken the resin and increase its viscosity, thereby increasing the drying rate and permitting the sculptograph to be framed (and therefore sold) faster than if a more liquid resin had been used.

4e. Aluminum and the Sculptograph

Analysis using XRF spectroscopy and SEM-EDS identified the metallic secondary support as a sheet of lead. No aluminum was detected using the XRF. In an attempt to detect elements of lower atomic weights, the XRF detector's filter was removed. Once again, aluminum was not detected (Table 1). A small sample of the secondary support was also studies using SEM-EDS. As this technique is carried out in a vacuum, it is capable of detecting lower molecular weight atoms such as aluminum. As seen in Figure 11, a small amount of aluminum was detected. As stated previously, the detection of silicon in conjunction with small amounts of aluminum suggests the presence of alumino-silicates, which are common contaminants of mined materials such as iron oxide and gypsum.

As stated previously in this paper, the sculptograph at the focus of this technical study has a label on the verso of the backing board identifying it as a *sculptograph*, "the genuine celebrated raised enlargements on Aluminum Metal. Naturally, this calls the accuracy of the label into question. If analysis has identified the secondary support as lead, why was the sculptograph advertised as being on aluminum metal?

As the term *sculptograph* was found in conjunction with three objects made by the Great Eastern Art Co., the term may have been a proprietary name. Other studios may have been producing similar objects with a different name. Claiming that the sculptograph was done on aluminum metal may have been an attempt by the Great Eastern Art Company to differentiate their bas-relief photograph from the competition.

Aluminum was not successfully extracted from ores until the second half of the 19th century, and the process did not become commercially viable until the late 1890s. During these fifty years, due to difficulty and cost of its extraction, aluminum metal was worth more than gold. Aluminum also gave the allusion of glamour: Emperor Napoleon III of France had his finest set of dishes made from aluminum (Skrabec 2006). As the metallic secondary support is not seen when the sculptograph is displayed, an expensive metal such as aluminum would not have been a practical secondary support. Aluminum would

not have been practical from a working point either: aluminum is quite strong and difficult to manipulate. Such a metal is opposite of what is recommended in 19th century patents (Hulbert 1898a,b). The characteristics of lead are ideal for the metallic component of a sculptograph.

The sculptograph was likely advertised as being on aluminum because having a photograph made of aluminum, the most expensive metal in the world, justifies a higher price for a sculptograph portrait. Having a sculptograph would be a status symbol: the owner could afford to have a photograph on "aluminum" where the aluminum serves a structural function and is not visible. This would have been a frivolous use of a highly precious metal.

5. Conclusions

Analysis conducted during this technical study indicate that all of the materials used in the creation of a sculptograph are consistent with the late 19th century, the estimated date of creation for the sculptograph in question. The primary paper support appears to consist of middle-to good quality bast fibers and the adhesive attaching the solar enlargement to the metallic secondary support is a gum-based adhesive. The pastels contain a gum binding medium and the following pigments: gypsum, calcium carbonate, barium sulfate, chrome yellow, Prussian blue, ultramarine blue, vermillion, and multiple iron oxide pigments. The filler material consists of inorganic pigments suspended within an organic matrix: a pine resin containing iron oxide, gypsum, calcium carbonate, and barium sulfate. The photographic component of the sculptograph was detected using XRF spectroscopy, and XRF spectroscopy and SEM-EDS identified the metallic secondary support as a sheet of lead. The identification of the metallic secondary support was lead contradicts a statement made of a label attached to the sculptograph.

The label on the verso states that a sculptograph is on a sheet of aluminum. Aluminum metal would be practical from neither a financial point nor a working point, and it is hypothesized that the statement was made to make the sculptograph a status symbol. This would enable a photography studio to charge a higher price for a sculptograph.

III. JOINT CONCLUSIONS

As objects, the ruby ambrotype and the sculptograph showcase the creativity and ingenuity of the 19th century photographers. When approaching the technical analysis of such objects, it is important to consult written primary sources such as contemporary periodicals, manuals, and patents in addition to the information gained through examination and analysis. All of this background is needed when considering the needs of the object, whether proper storage and display requirements or designing a treatment approach. In summary, in order to competently approach an object, all aspects of that object must be thoroughly understood.

IV. REFERENCES

PART ONE: RUBY AMBROTYPES

Anthony's bulletin of photography, invention and improvement. 1857. New York, NY: Holman (printer). [Hagley Museum and Library, Wilmington, DE]

Baade, B. 2008. Personal Communication. Winterthur/University of Delaware, Newark, DE.

Biser, B. 1899. *Elements of glass making*. Pittsburgh, PA: Glass and Pottery Pub. Co.

Burgess, N.G. 1858 4th ed. *The photograph and ambrotype manual: a practical treatise*. New York, NY: Wiley and Halsted.

Fedotieff, P. and A. Lebedeff. 1924. Über die absorptionspektra van gefärbten gläsern. *Zeitschrift für anorganiche und allgemeine Chemie*. 134 (1): 87-101.

Green, L.R. and F. A. Hart. 1987. Colour and chemical composition in ancient glass: an examination of some Roman and Wealden glass by means of ultraviolet-visible-infrared spectrometry and electron microprobe analysis. *Journal of Archaeological Science* 14: 271-282.

Humphrey's Journal. 1857. Positive Collodion Process. *Humphrey's Journal* 9(4).

McCabe, C. 1991. Preservation of 19th Century negatives in the National Archive. *Journal of the American Institute of Conservation* 30(1):41-73.

McGlinchey, C and C. Maines. 2005. Chemistry and Analysis of coating materials. In *Coatings on Photographs*. Ed. C. McCabe et al. Washington, D.C.: American Institute for Conservation.

McCormick-Goodhart, M. 1990. The multilayer structure of tintypes. *ICOM Committee for Conservation preprints*. 9th Triennial Meeting, Dresden, GDR. Paris: ICOM. 1:262-267.

Moor, I. 1976. The ambrotype—research into its restoration and conservation Part 1. *The paper conservator*. 1: 22-25.

Moor I. 1976. The ambrotype—research into its restoration and conservation Part 2. *The paper conservator* 2: 36-43.

Newhall, B. 1958. Ambrotype, a short and unsuccessful career. *Image*. International Museum of Photography at the George Eastman House. 7(8): 171-177.

Nishimura, D. 2008. Personal communication. Image Permanence Institute. Rochester, NY.

Osterman, M. 2007. Personal communication. Scully & Osterman Studio and George Eastman House, Rochester, NY.

Osterman, M. and G. Romer. 2007. History and evolution of photography. In *Focal Encyclopedia of Photography 4th edition*. Ed Peres, M. et al. Amsterdam: Elsevier.

Weyl, W.A. 1976. *Coloured Glass*. Sheffield, England: Society of Glass Technology.

PART TWO: SCULPTOGRAPHS

Albright, G. E. and M. K. Lee. 1989. A short review of crayon enlargements: history, technique, and treatment. *Topics in photographic preservation* 3: 28-36.

Burgio, L., and R. Clark. 2001. Library of FT-Raman spectra of pigments, minerals, pigment media and varnishes. *Spectrochimica Acta* Part A 57(7): 1491-1591.

Chinn, R. H. and J. L. McGee. 1874. Improvement in photographic pictures. U.S. Patent 153,048. Assigned to Richard H. Chinn and John L. McGee, Washington, D.C.

Enyeart, J. L., A. B. Anderson, S. J. Perron, D. K. Rollins, and Q. Fernando. 1983. Non-destructive elemental analysis of photographic paper and emulsions by X-ray fluorescence spectroscopy. *History of photography* 7: 99-113

Flomaton Antique Auction. 2007. www.flomatonantiqueauction.com. (Accessed 11/14/07).

Gettens, R. J. and G. L. Stout. [1942] 1966. *Painting materials: a short encyclopaedia.* New York: Dover Publications, Inc.

Hulbert, D. F. 1898. Relief-photograph and method of producing the same. U.S. Patent 615,025. Assigned to Duran F. Hilbert, St. Louis, Missouri.

Hulbert, D. F. 1898. Embossing photographs. U.S. Patent 615,026. Assigned to Duran F. Hilbert, St. Louis, Missouri.

Low, M. J. D. and N. S. Baer. 1977. Application of infrared Fourier transform spectroscopy to problems in conservation. Part 1, general principles. *Studies in conservation* 22(3): 116-128.

Mastro Auctions. 2005. www.mastronet.com. (Accessed 11/14/07).

McCabe, C. and L. D. Glinsman. 1995. Understanding Alfred Stieglitz' platinum and palladium prints: examination by X-ray fluorescence spectrometry. *Research Techniques in Photographic Conservation. Proceedings from the Copenhagen Conference.* Copenhagen, Denmark. 31-40.

Reilly, J. M. 1986. *Care and identification of 19th-century photographic prints.* Rochester: Kodak.

Skrabec, Quentin R., Jr. 2006. *The metallurgic age: the victorian flowering of invention and industrial science.* Jefferson: McFarland & Company, Inc.

University College of London. 2008. Raman Spectroscopic Library of Natural and Synthetic Pigments. www.chem.ucl.ac.uk/resources/raman/index.html. (Accessed 2/1/2008).

V. ACKNOWLEDGEMENTS

Professor in Art Conservation), Jae Gutierrez (UD Assistant Professor in Art Conservation), Barb Lemmen (UD Adjunct Assistant Professor in Art Conservation). And finally thanks to the many photograph conservators and experts consulted during the course of this project, of whom there are too many to be named individually.
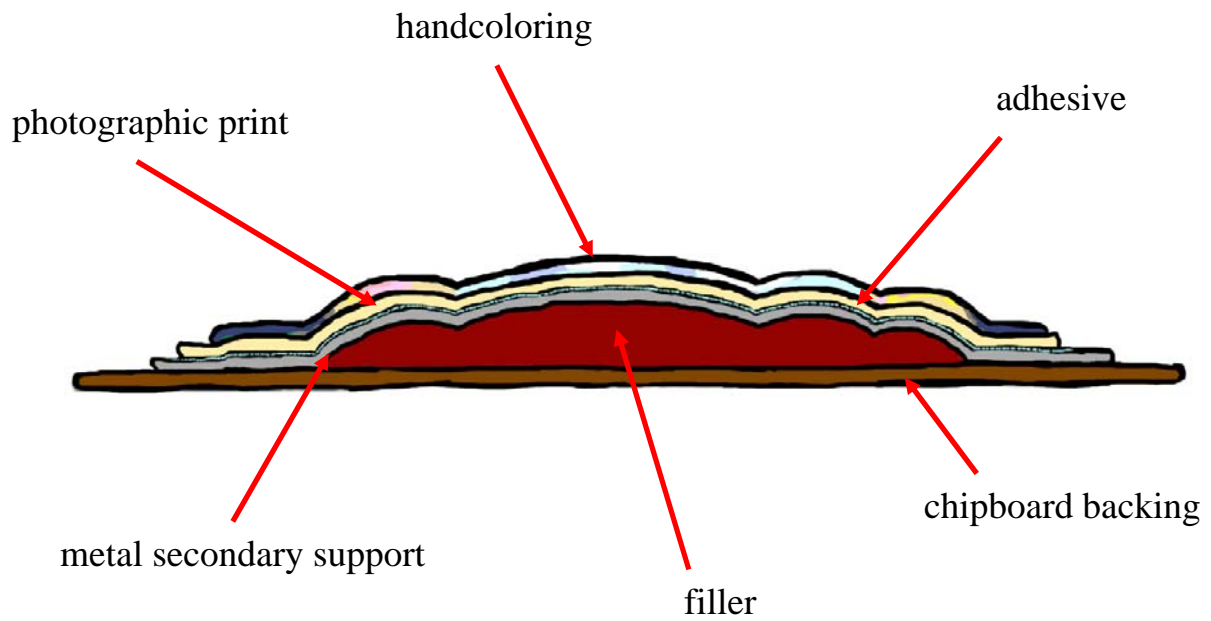
VI. APPENDECIES

PART ONE: RUBY AMBROTYPES

Appendix 1: Black Glass Recipes

Common Glass:	
Green Cullet………………100	**Manganese………………8**
Soda………………………..38	Oxide of Iron……....…….6
Lime…………………………18	Pulverized coke………….4
Arsenic……..……………….2	
Fine Glass:	
Sand………………………..100	Oxide of copper…………10
Potash………………………36	Oxide of iron…………….10
Lime………………………..13	**Manganese ..…………….10**
Zaffre………………………10	
Sand……………………….100	Oxide of copper………….4
Potash……………………...15	Oxide of iron……………..4
Soda………………………..24	**Manganese………………5**
Lime………………………18	Zaffre…………………….2

Biser, B. 1899. *Elements of Glass and Glassmaking*. Pittsburgh, PA: Glass and Pottery Publishing Co.

PART TWO: SCULPTOGRAPHS

Appendix 1: Cross Section of a Sculptograph

handcoloring

adhesive

photographic print

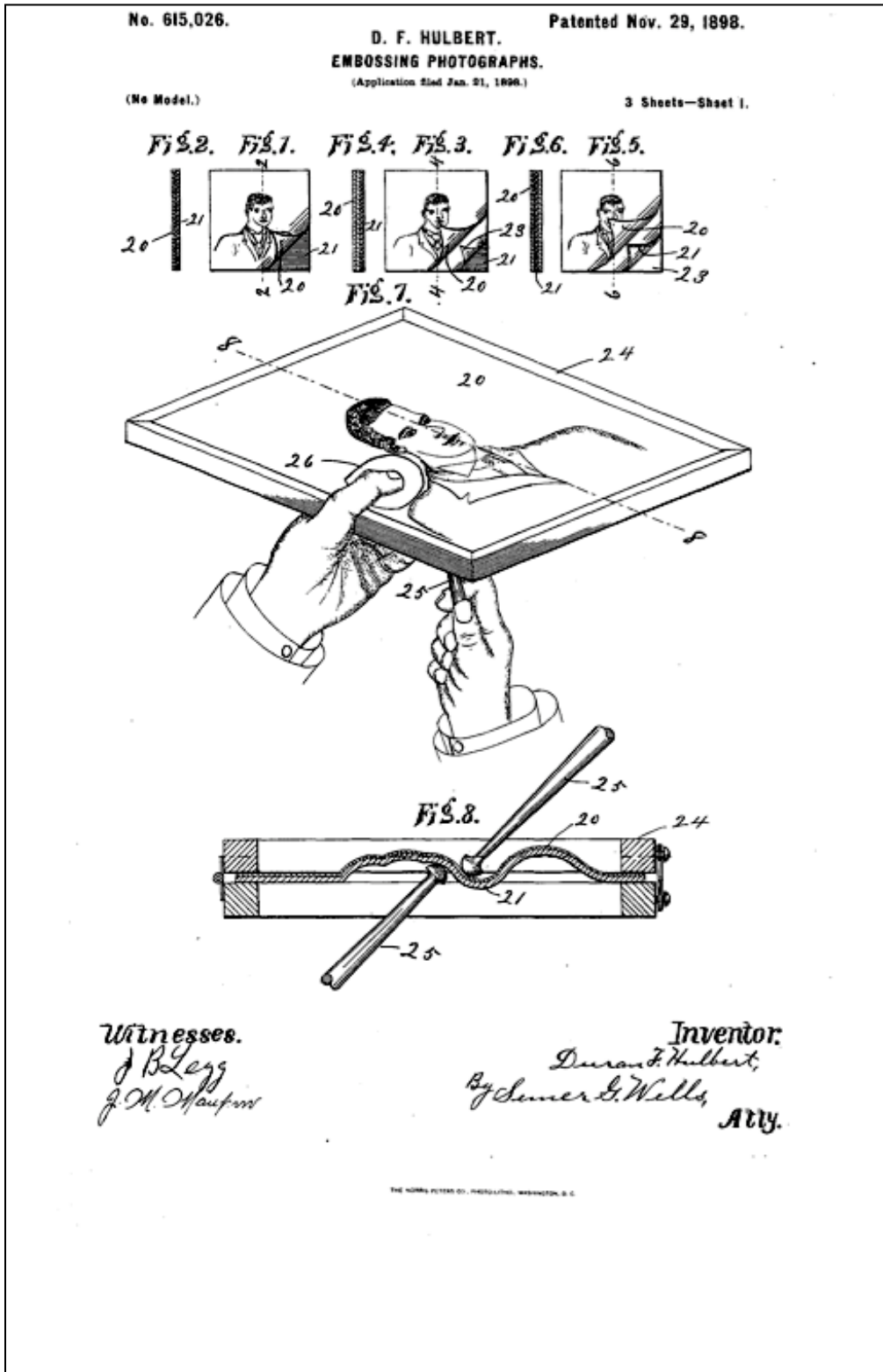metal secondary support

filler

chipboard backing

Appendix 2: *Relief Photograph and Method of Producing the Same*

U.S. Patent 615,025, Assigned to Duran F. Hulbert in 1989
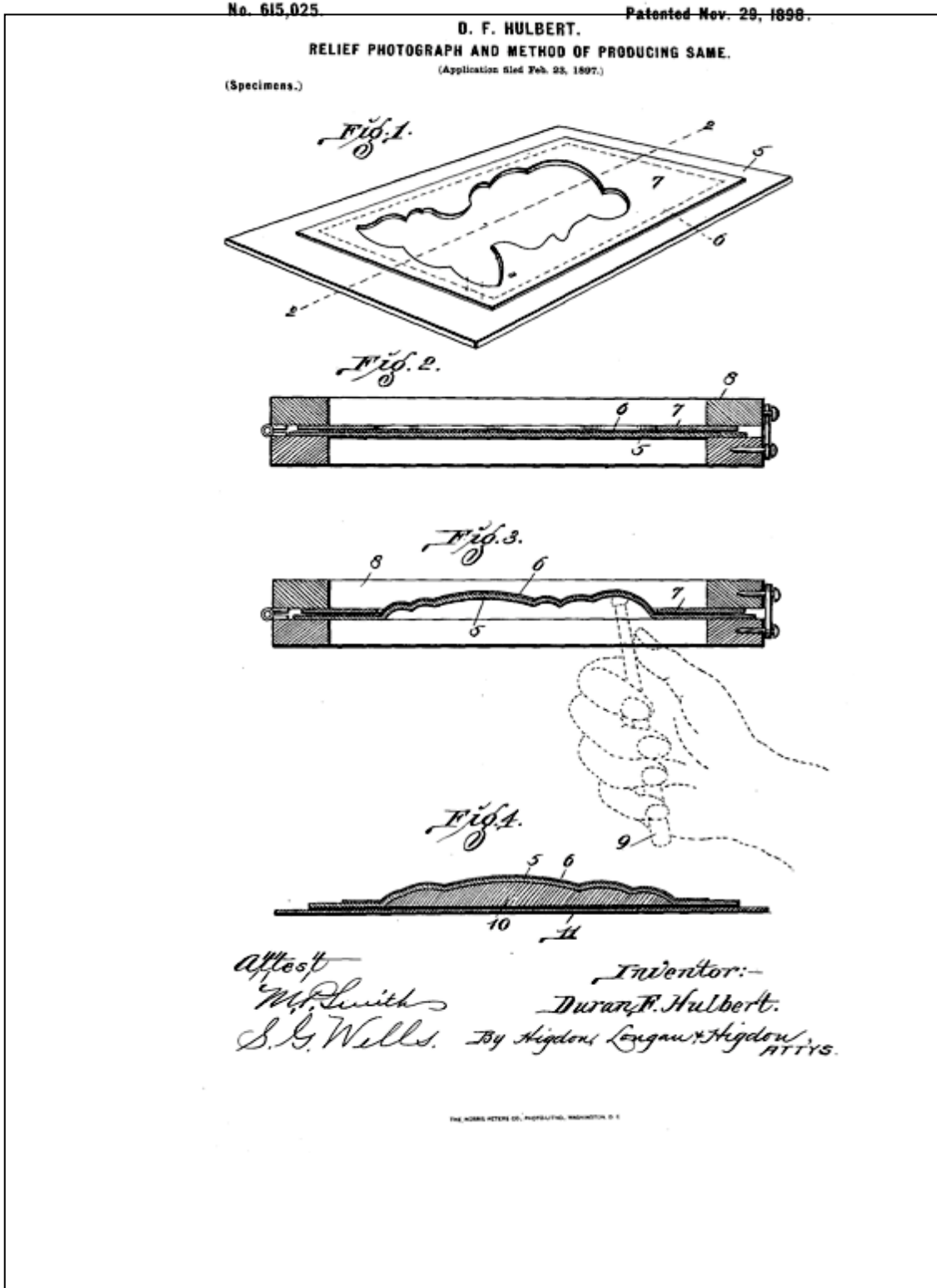
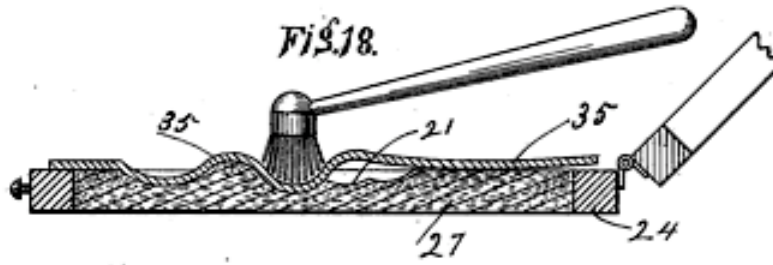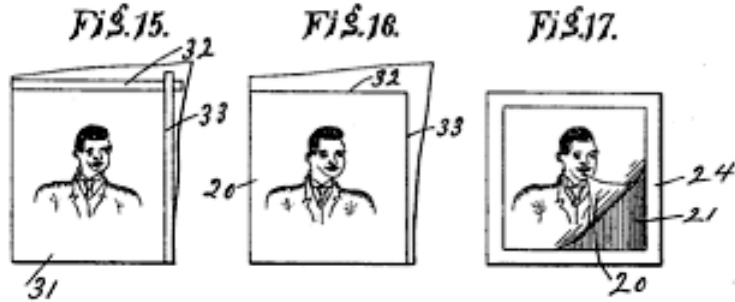## U.S. Patent 615,026, Assigned to Duran F. Hulbert in 1989

No. 615,026.

D. F. HULBERT.
EMBOSSING PHOTOGRAPHS.
(Application filed Jan. 21, 1898.)

Patented Nov. 29, 1898.

(No Model.)

3 Sheets—Sheet 3.

Fig.15.

Fig.16.

Fig.17.

Fig.18.

Fig.19.

Witnesses.
J B Legg
J. M. Maupin

Inventor
Duran F Hulbert,
By Semer G. Wills
Atty

Appendix 3: Sample Locations

AL 5067, Sculptograph

Sample Locations

Scraping removed for FTIR/Raman analysis

Location of XRF analysis

Loose fragment removed for GC-MS/SEM-EDS analysis

Location of PLM fiber sample